| REPORT DOCUMENTATION PAGE | | READ INSTRUCTIONS BEFORE COMPLETING FORM |
|---|---|---|
| 1. REPORT NUMBER<br>Technical Report GL-79-8 | 2. GOVT ACCESSION NO. | 3. RECIPIENT'S CATALOG NUMBER |
| 4. TITLE (and Subtitle)<br><br>ANALYSIS OF GRID CELL REINFORCED PAVEMENT BASES | | 5. TYPE OF REPORT & PERIOD COVERED<br>Final Report |
| | | 6. PERFORMING ORG. REPORT NUMBER |
| 7. AUTHOR(s)<br>James K. Mitchell<br>T-C. Kao<br>Edward Kavazanjian, Jr. | | 8. CONTRACT OR GRANT NUMBER(s)<br>Contract No.<br>DACA39-78-M-0161 |
| 9. PERFORMING ORGANIZATION NAME AND ADDRESS<br>Department of Civil Engineering<br>University of California<br>Berkeley, Calif. 94720 | | 10. PROGRAM ELEMENT, PROJECT, TASK AREA & WORK UNIT NUMBERS<br>Project No. 4A161102AT22<br>Task A2, Work Unit 007 |
| 11. CONTROLLING OFFICE NAME AND ADDRESS<br><br>Office, Chief of Engineers, U. S. Army<br>Washington, D. C. 20314 | | 12. REPORT DATE<br>July 1979 |
| | | 13. NUMBER OF PAGES<br>66 |
| 14. MONITORING AGENCY NAME & ADDRESS(If different from Controlling Office)<br>U. S. Army Engineer Waterways Experiment Station<br>Geotechnical Laboratory<br>P. O. Box 631, Vicksburg, Miss. 39180 | | 15. SECURITY CLASS. (of this report)<br><br>Unclassified |
| | | 15a. DECLASSIFICATION/DOWNGRADING SCHEDULE |

16. DISTRIBUTION STATEMENT (of this Report)

Approved for public release; distribution unlimited.

17. DISTRIBUTION STATEMENT (of the abstract entered in Block 20, if different from Report)

18. SUPPLEMENTARY NOTES

19. KEY WORDS (Continue on reverse side if necessary and identify by block number)
Base courses
Grid cells
Pavements
Reinforcing materials
Subbases

20. ABSTRACT (Continue on reverse side if necessary and identify by block number)

The full-scale field tests conducted at the U. S. Army Engineer Waterways Experiment Station (WES) have shown that interconnected shallow, thin-walled cells placed over a soft subgrade, with the cell axes oriented vertically, and filled with sand can provide significantly greater load-carrying capacity than can the compacted soil alone. Laboratory model tests have established some of the influences of (1) the ratio of loaded area radius to cell width, (2) the ratio of cell depth to cell width, (3) the subgrade thickness, and (4) repeated
(Continued)

DD FORM 1 JAN 73 1473 EDITION OF 1 NOV 65 IS OBSOLETE

20. ABSTRACT (Continued).

loading. The results of these investigations demonstrated clearly that grid cell systems may provide an economical, easily constructed, and effective expedient pavement structure.

Accordingly, this study was undertaken to investigate in further detail the behavior of grid cell systems, with particular reference to failure mechanisms and analytical approaches to design. The possible grid cell failure modes analyzed included (1) cell penetration of the subgrade, (2) cell bursting, (3) cell wall buckling, (4) bearing capacity, (5) bending, (6) durability failure, and (7) excessive rutting.

# PREFACE

The investigation reported herein was sponsored by the Office, Chief of Engineers (OCE), U. S. Army, as part of Project 4A161102AT22, Task A2, Work Unit 007, "Analysis of Grid Cell Reinforced Bases and Subbases for Pavements and Foundations." This work was performed for the U. S. Army Engineer Waterways Experiment Station (WES) under Contract No. DACA39-78-M-0161 by Messrs. J. K. Mitchell, T-C. Kao, and E. Kavazanjian, Jr., Department of Civil Engineering, University of California, Berkeley, California.

The WES personnel directly concerned with this project were Messrs. J. P. Sale, Chief, Geotechnical Laboratory (GL); R. G. Ahlvin, Assistant Chief, GL; H. H. Ulery, Jr., Chief of Pavement Design Division; and Dr. G. M. Hammitt, Design Criteria Branch, GL. The OCE Technical Monitor for this project was Mr. S. S. Gillespie.

Director of the WES during the conduct of this investigation was COL J. L. Cannon, CE. Technical Director was Mr. F. R. Brown.

# CONTENTS

# CONVERSION FACTORS, U. S. CUSTOMARY TO METRIC (SI)
## UNITS OF MEASUREMENT

U. S. customary units of measurement used in this report can be converted to metric (SI) units as follows:

| Multiply | By | To Obtain |
|---|---|---|
| inches | 25.4 | millimetres |
| pounds (force) | 4.448222 | newtons |
| pounds (force) per inch | 175.1268 | newtons per metre |
| pounds (force) per square inch | 6.894757 | kilopascals |
| pounds (force) per square inch per inch | 0.27144 | kilopascals per millimetre |
| pounds (mass) | 0.4535924 | kilograms |
| pounds (mass) per cubic foot | 16.01846 | kilograms per cubic metre |
| pounds (mass) per cubic inch | 27,679.9 | kilograms per cubic metre |
| square inches | 645.16 | square millimetres |

# ANALYSIS OF GRID CELL REINFORCED PAVEMENT BASES

by

James K. Mitchell, T-C. Kao and Edward Kavazanjian, Jr.

## INTRODUCTION

Full scale field tests at the U. S. Army Engineer Waterways Experiment Station (WES) have shown that interconnected shallow, thin-walled cells placed over a soft subgrade, with the cell axes oriented vertically, and filled with sand can provide significantly greater load carrying capacity than can the compacted soil alone (Webster and Watkins, 1977; Webster and Alford, 1978). Laboratory model tests by Rea and Mitchell (1978) have established some of the influences of (1) the ratio of loaded area radius (a) to cell width (B), (2) the ratio of cell depth (h) to cell width (B), (3) the subgrade stiffness (k), and (4) repeated loading. A schematic diagram of the systems studied in these investigations is shown in Fig. 1.

The results of these investigations have demonstrated clearly that grid cell systems may provide an economical, easily constructed, and effective expedient pavement structure. Accordingly, the present study was undertaken at the request of WES to investigate in further detail the behavior of grid cell systems. Of particular interest were failure mechanisms and the development of analytical approaches for the design of

grid cell systems.  This report presents the results of this study.

SIGNIFICANT FINDINGS FROM PREVIOUS INVESTIGATIONS

Field Tests

Full scale traffic field tests under controlled conditions at WES (Webster and Watkins, 1977; Webster and Alford, 1978; Webster - personal communication, 1978) have established several aspects of sand filled grid cell performance pertinent to their design.

1.  For systems of rectangular aluminum cells (6-in. and 12-in. grids, 6-in. and 12-in. high; with a 2-in. crushed stone surfacing) permanent surface depressions and rut depths increased slightly more than pro-portionally with the logarithm of the number of coverages for rut depths less than 3 to 4 inches.  Complete failure then developed rapidly with increased numbers of coverages.  This rapid failure may have been accelerated by removal of the crushed stone cover layer and sand displacement from the cells which led to direct loading of exposed cell walls.

2.  Resilient grid deflections are not great, and the behavior resembles that of a slab.

3.  The density of the sand in the cells is important, with higher density giving improved performance.

4.  The performance of sand-filled grid cells when used over very soft sub-grades may be equivalent to that of a layer of crushed stone that is as much as 1.6 times thicker than the height of the cells.

2

5. Sand surfacing over grid cells does not perform satisfactorily under traffic. The sand is easily displaced from over the cells causing direct application of wheel loads to the top of the grids, which, in turn, fail by buckling and bending. These failures do not develop when a 2-in. thick gravel layer is used.

6. Failure of aluminum grid cell systems was exhibited in several ways:

    a. Eruption of cells at the surface adjacent to the wheel path (Webster and Alford, 1978: Photo 15).

    b. Penetration of cells into the subgrade (Webster and Alford, 1978: Test Item 3).

    c. Shear of grid layer along the outside edge of the wheel path (Webster and Alford, 1978: Photo 23).

    d. Cutting of an underlying membrane reinforcement by cell edges (Webster and Alford, 1978: Photo 27).

7. Currently available paper grid cells disintegrate on wetting.

8. Impervious cell walls prevent lateral drainage.

Laboratory Model Tests

Laboratory model tests using sand-filled paper grid cells (B = 2 inches, paper thickness = 0.008 inch) over a spring base subgrade with static and repeated plate loading at the surface indicated the following (Rea and Mitchell, 1978).

1. Failure was generally sudden and well-defined in static load tests and occurred because of rupture of the reinforcing. Failure by tearing from the bottom along glued joints between cells was observed in some

cases.  Abrupt failure was not observed in the repeated load tests.

2.  Maximum bearing capacity under static load was found for a loaded area
radius to cell width ratio a/B in the range of 0.75 to 1.0.

3.  The optimum value of the ratio of cell height to width h/B was about
2.25.

4.  The ultimate bearing capacity of the grid cell system increased with
increasing subgrade stiffness.

5.  Grid cell reinforcement offered greatly improved resistance to repeated
loads.

6.  Repeated loading causes sand to bounce out of grid cells that are
unprotected by a cover layer.

## GRID CELL FAILURE MODES

From considerations of available test results and evaluation of
possible sand-cell-subgrade interaction mechanisms, several possible modes
of failure have been identified.

1.  Cell Penetration

Cells push downward relative to the sand they contain into the
soft subgrade below.  If a fabric membrane layer is used beneath the
cells, it may be cut by the cell edges and corners.  The performance of
test item 3 and photograph 27 of Webster and Alford (1978) are illustrative
of this.

4

2. Cell Bursting

   The stresses exerted by the sand within a cell exceed its bursting
   strength. This mode of failure seems possible only if the loaded area
   is contained entirely within a single cell.

3. Cell Wall Buckling

   This mode of failure will develop if there is insufficient lateral
   restraint for the cell walls and the cell walls are directly loaded.
   If sand is displaced from the cells, bending and buckling of the cell
   walls generally develop rapidly.

4. Bearing Capacity

   The stiffness and load-distributing characteristics of the sand-
   filled grid cells are inadequate to prevent shear failure of the under-
   lying soft soil.

5. Bending Failure

   The reinforced sand appears to behave as a slab. If excessive
   wheel loads are applied, then failure in bending could result, with
   the grid cells tearing apart at the bottom.

6. Durability Failure

   The grid cells deteriorate as a result of prolonged exposure to
   air, water, and sunlight. Durability failure can be prevented by proper
   choice of materials.

7. Excessive Rutting

   Excessive permanent deformations develop after large numbers of
   load repetitions, and loss of serviceability results. All of the above

failure modes may be developed to some degree. As is true for conventional pavement structures, rational analysis and prediction of rut formation and development is extremely difficult if not impossible at the present time. Nonetheless, it appears from the limited field test data available that rut formation is the major mode of distress for rut depths up to about 3 to 4 inches. Complete failure of the system generally ensues quickly thereafter.

Although analysis leading to a suitable prediction for the accumulation of permanent deformation as a function of number of coverages has not yet been possible, a reasonable approach may be to limit the resilient or elastic deformations of the grid cell layer and the subgrade. Alternatively, limiting the shear stresses and vertical compressive stresses in the subgrade may serve the same purpose.

Each of these failure modes is examined in greater detail in the following sections of this report.

## ANALYSIS OF FAILURE BY PENETRATION

Because the grid cell walls are stiffer than the sand that they contain, they will tend to carry a higher vertical stress intensity from the applied loads than the sand. If the downward force is greater than can be resisted by the friction between the sand and vertical cell surfaces, then downward penetration will occur. Some added resistance to penetration will be provided by the bearing capacity of the bottom edges of the cell walls. This resistance will be small, however, owing to the small wall thickness, and it is neglected here.

Consider a square grid cell with height h and width B as shown in Fig. 2. The unit frictional resistance f on the interior of the cell walls at depth z is

$$f = \sigma_h \tan\delta \tag{1}$$

where $\sigma_h$ is the horizontal stress and $\delta$ is the mobilized friction angle between the cell wall and sand. The value of $\sigma_h$ depends on the coefficient of lateral earth pressure K according to

$$\sigma_h = K\sigma_v \tag{2}$$

where $\sigma_v$ is the vertical stress at depth z.

The vertical stress within the cell $\sigma_v$ at any depth z will depend on $\sigma_o$, the average vertical stress at the surface of the sand, plus the weight of the sand above z, less some stress $\sigma_f$ which reflects the transfer of some vertical load to the cell walls by friction above depth z. For a horizontal slice of thickness dz at depth z within the grid cell as shown in Fig. 2b, vertical force equilibrium gives an equation for change in vertical stress with depth,

$$d\sigma_v\, B^2 = -B^2\gamma\, dz + 4Bf\, dz \tag{3}$$

where $\gamma$ is the unit weight of the sand. Because the influence of the unit weight of sand will be small, it may be neglected, so equation (3) becomes

$$d\sigma_v = \frac{4K\sigma_v \tan\delta}{B}\, dz \tag{4}$$

or

$$\frac{d\sigma_v}{\sigma_v} = \frac{4K \tan\delta}{B}\, dz \tag{5}$$

7

Integration gives

$$\ln \sigma_v = \frac{4K \tan\delta}{B} z + c \tag{6}$$

At $z = 0$, $\sigma_v = \sigma_o$, where $\sigma_o$ is the vertical stress transmitted to the sand at the surface.

Thus $c = \ln \sigma_o$, and equation (6) can be written

$$\ln \left(\frac{\sigma_v}{\sigma_o}\right) = \frac{4K \tan\delta z}{B} \tag{7}$$

or

$$\sigma_v = \sigma_o e^{4K\tan\delta z/B} \tag{8}$$

Equation (8) gives the average vertical stress at some depth z within a grid cell filled with cohesionless, weightless soil as a function of lateral earth pressure coefficient K and mobilized friction $\tan\delta$ between the grid cell wall and soil.

Substitution of equation (8) into equation (1) gives an expression for the unit frictional resistance developed on the grid wall at some depth z.

$$f = K\tan\delta\sigma_o e^{4K\tan\delta z/B} \tag{9}$$

The frictional resistance of the slice in Fig. 2b will be

$$\bar{f} = 4Bfdz = 4BK\tan\delta\sigma_o e^{4K\tan\delta z/B} dz \tag{10}$$

The total frictional resistance of the cell, F, is obtained by integrating $\bar{f}$ over the cell height h, or

$$F = \int_o^h \bar{f} \tag{11}$$

8

$$F = \int_0^h 4BK\tan\delta\sigma_o e^{4K\tan\delta z/B} \, dz \tag{12}$$

Integration of equation (12) gives

$$F = B^2\sigma_o e^{4K\tan\delta z/B} \Big|_0^h \tag{13}$$

Substitution of the limits gives

$$F = B^2\sigma_o \left( e^{4K\tan\delta h/B} - 1 \right) \tag{14}$$

If $\delta$ is set equal to $\delta_m$, the maximum attainable friction angle between the soil and the cell wall, the maximum value of F; i.e., the penetration resistance of the cell, is obtained.

$$F_{max} = B^2\sigma_o \left( e^{4K\tan\delta_m h/B} - 1 \right) \tag{15}$$

Equation (15) is slightly conservative in that it does not include the resistance to penetration that would be provided by the body forces acting on the sand due to gravity (the $B^2\gamma dz$ term in equation (3)). It does, however, provide a basis for illustrating the influences of system parameters on $F_{max}$ and for estimating the cell dimensions for different conditions.

Equation (15) shows that for a given ratio of cell height to width, $h/B$, the penetration resistance increases in proportion to the vertical stress at the surface and as the square of the cell width. Because $F_{max}$ increases exponentially with $h/B$, however, it is clear that an increase in B without a proportional increase in h can give a reduction in penetration resistance.

9

Field tests have shown that the performance of grid cells is improved when the sand fill is densified. That densification should give increased resistance to penetration is indicated in equation (15) by the exponential dependence of $F_{max}$ on K, the lateral pressure coefficient, which increases with increased density. In addition densification may result in higher values of $\delta_m$.

The direct dependence of $F_{max}$ on $\sigma_o$ indicates the great importance of the vertical stress distribution between the cell walls and the sand within them. Unless a stress-distributing cover layer is used, the cell walls, being stiffer than the sand, will carry a high proportion of the stress and $\sigma_o$ will be small, giving low penetration resistance. Use of a thin cover layer, however, should insure that $\sigma_o$ is high enough that adequate penetration resistance can be developed. In the field tests done at the Waterways Experiment Station (Webster and Alford, 1978) a 2-inch gravel layer was used over the grid cells, and this appeared, in most cases, to be sufficient to provide adequate $\sigma_o$ for the needed penetration resistance.

In most of the WES tests grid cells were 12-in. high by 6-in. wide, so h/B = 2. If it is assumed that the vertical wheel load was distributed uniformly over the tire imprint area, $\sigma_o$ would be 70 psi. Let it be further assumed that K was 0.9 and $\delta_m$ was 20° (sand against polished aluminum). Then, according to equation (15)

$$F_{max} = 6^2 \times 70 \left( e^{4X.9Xtan20X2} - 1 \right) = 36 \times 70 \times 12.74$$

$$F_{max} = 32,114 \text{ lb.}$$

Thus for these conditions failure by penetration of the grid cells would not be anticipated under the 4000 to 5000 lb. wheel loads used in

10

the WES tests, even if the full load was carried by a single cell.

For one of the items used in the WES tests 6-in. high cells were used, so that $h/B = 1$. For this case equation (15) gives $F_{max} = 6822$ lb., a penetration resistance only slightly greater than the wheel loads.

In actuality the penetration behavior of grid cells under repeated traffic loadings should be somewhat more complex than indicated by the preceding simple analysis. The most critical conditions probably arise when the wheels pass directly over the joints connecting the cells. Each time the load passes the grid will deflect downwards relative to the sand by a small amount. Because of the large frictional resistance between sand and cell wall and because of grid flexibility, the recovery of the original shape will not be complete, and ruts may gradually form.

In some grid cell tests the grid mat has been underlain by fabric reinforcement. Although the performance of the membrane-reinforced layer has been somewhat better than that of grid cell systems without underlying membranes, cell penetration can cut the membrane (Webster and Alford, 1978, Photo 27). Unfortunately, to provide significant reinforcement a membrane must be under tension, and the greater the tension in a membrane, the easier it is to penetrate by a cutting edge such as the edge of a metal grid cell. It could be, therefore that metal grid cells and fabric membranes may not be a compatible combination.

## ANALYSIS OF CELL FAILURE BY BUCKLING

Wall buckling is a soil-structure interaction problem that could possibly be analyzed by numerical methods; for example, by a plane strain or axisymmetric analysis of a thin sheet surrounded by soil. Both laboratory

and field tests have shown, however, that buckling is most likely to occur only when the cell walls are unprotected and are subjected to directly applied vertical loads. In those instances when the tops of the cells are covered by a sand or gravel layer and the tops do not become exposed, buckling has not occurred. Consequently, one solution of the buckling problem is to prevent direct load application to the tops of cell walls.

## ANALYSIS OF CELL FAILURE BY BURSTING

Two approaches have been used to estimate the vertical stress required to cause bursting of a grid cell. The critical condition for cell bursting would be the case of a loaded area that is contained entirely within the plan area of a single grid cell as shown in Fig. 3. Under this condition the sand in the adjacent cells will not be confined by a vertical stress, so the passive restraint available to the loaded cell will be small.

The forces at failure acting on a single cell assumed loaded uniformly over its entire surface area can be considered. An active lateral pressure condition will be developed within the loaded cell. This will be resisted by the passive resistance offered by the sand in adjacent cells and by tension in the cell walls and joints. There may also be some restraint offered by friction between the expanding cell and the underlying base. The high lateral stresses within a single loaded cell will tend to cause it to distort to a circular shape. At failure the stresses and forces will be as indicated in plan in Fig. 4. In a vertical section the forces are as indicated in Fig. 5.

Horizontal force equilibrium gives

12

$$P_p \left(\frac{4B}{\pi}\right) \cos\delta - P_a \left(\frac{4B}{\pi}\right) \cos\delta + F_t \left(\frac{4B}{\pi}\right) + F_b \left(\frac{4B}{\pi}\right) + 2Th = 0 \qquad (16)$$

$$(P_p - P_a) \cos\delta + F_t + F_b + \frac{2\pi Th}{4B} = 0 \qquad (17)$$

The terms in equation (17) can be estimated according to

$$P_a = K_a \cdot h \cdot \left(\sigma_o + \frac{\gamma h}{2}\right) \qquad (18a)$$

$$P_p = K_p \cdot h \cdot \left(\frac{\gamma h}{2}\right) \qquad (18b)$$

$$F_t = \mu N_t \qquad (18c)$$

$$F_b = \mu N_b \qquad (18d)$$

$T$ = tearing strength of cell wall or joint (force/length)

where      $K_a$ = coefficient of active earth pressure

$K_p$ = coefficient of passive earth pressure

$\gamma$ = unit weight of sand

$\mu$ = coefficient of friction between edge of cell wall and overlying or underlying soil layer

$N_t$ = vertical force on top of cell wall

$N_b$ = vertical force at bottom of cell wall.

In a typical grid cell system the walls will be flexible and may also penetrate into the overlying and underlying layers. Accordingly, the forces $F_t$ and $F_b$ are not likely to be of significant magnitude and will be neglected.

Substitution of equations (18a) and (18b) into equation (17) gives

$$\left(K_p \frac{\gamma h}{2} - K_a \frac{\gamma h}{2} - K_a \sigma_o\right) \cos\delta + \frac{\pi T}{2B} = 0 \qquad (19)$$

13

Solving for $\sigma_o$, the vertical pressure on the top of the sand required to cause cell bursting, gives

$$\sigma_o = \frac{\frac{\pi T}{2B} + \frac{\gamma h}{2}(K_p - K_a)\cos\delta}{K_a \cos\delta} \tag{20}$$

Consider a sand fill with $\phi = 35°$. Then $K_a = 0.27$ and $K_p = 3.69$ according to the Rankine theory. If $\gamma = 110 \text{ lb/ft}^3 = 0.0636 \text{ lb/in}^3$ and $\delta = 20°$, then

$$\sigma_o = \frac{\frac{1.57T}{B} + .0318h(3.69 - 0.27)\cos 20°}{0.27\cos 20°}$$

$$\sigma_o = 6.19\frac{T}{B} + 0.40h \quad \text{(psi)} \tag{21}$$

for T in lb/in., B in in., and h in in..

Equation (21) shows that the allowable vertical stress varies directly as the tearing strength of the cell material or connecting joint between cells and inversely as the cell width, B. The second term on the right hand side of equation (21) is small and can be neglected.

For aluminum grid cells of the type used by Webster and Alford (1978) B = 6 in. and $\sigma_o$ was 70 psi. The required tear strength according to equation (21) would be

$$T = \frac{70 \times 6}{6.19} = 67.8 \text{ lb/in.}$$

Although this appears reasonable for aluminum cell material, a single available laboratory test result using paper grid cells gave the following result:

14

Tear strength of cell (joint failure) = 1.32 lb/in

B = 2 inches

$\sigma_o$ according to equation (21)    = 4 psi

$\sigma_o$ measured to cause cell bursting    = 72 psi.

It appears, therefore, that the simple analysis leading to equation (21) gives an unreasonably low estimate of the bursting strength. Accordingly, a second method of analysis was developed as follows.

In this second approach an attempt is made to account for the various displacements that must occur for the cells to burst and the loaded area to displace downwards. Furthermore it recognizes that because of the inter-connection of cells, distortion to a circular shape before failure is not probable. As in the first approach, it is recognized that bursting failure is probable only if the loaded area is fully contained within a single cell.

The total bearing capacity can be separated into four parts as shown in Fig. 6. These contributions are

1. The bearing capacity of the sand layer in the absence of reinforcement, $\sigma_1$.

2. The resistance to overcome the strength of the cell walls in tearing or to fail joints between cells, $\sigma_2$.

3. The resistance to displacement of the sand in adjacent cells relative to the cell walls, $\sigma_3$.

4. The resistance to downward displacement of sand in the loaded cell contributed by friction between the sand and cell walls, $\sigma_4$.

15

The magnitudes of these contributions can be estimated approximately as follows. An example is also given which compares the computed value of $\sigma_o$ to cause cell rupture with the value measured in a model test. In this test square paper grid cells were 4-in. high and 2-in. wide. The circular loading plate was 2-in. in diameter, and the sand-filled cells were founded on a spring base having a stiffness $k = 50$ psi/in.

1.  The bearing capacity of the unreinforced layer can be estimated using conventional bearing capacity theory, or it may be separately measured. For the example a value of 27.2 psi was directly measured.

2.  The resistance due to cell tearing or joint failure depends on the strength of the cell material. For the paper grid cells tested the tearing stress was 1.32 lb/in, and failure occurred at the joints connecting adjacent cells. The vertical stress required to cause tearing of a sand-filled cell can be estimated with the aid of Fig. 7 and the assumption that the weight of sand in the cells is negligible.

    Equilibrium of horizontal forces acting on an element $\Delta$ high requires

    $$K_A \times \sigma_2 \times \Delta \times 2" \times 2 \text{ sides} \times \sin 45° = 2T = 2 \times 1.32 \times \Delta \qquad (22)$$

    For $K_A = 0.3$

    $$0.3\sigma_2 \times 4 \times .707 = 2.64$$

    $$\sigma_2 = 3.1 \text{ psi.}$$

3.  The resistance to displacement of the sand in adjacent unloaded cells owing to friction between the sand and cell walls will be negligible because of the absence of overburden or significant confining pressure, so it can be neglected; i.e., $\sigma_3 \approx 0$.

16

4. The resistance to downward displacement of sand in the loaded cell due to friction along the side walls can be estimated with the aid of Fig. 8. Fig. 8a shows shear bearing capacity failure geometry in relation to the cell walls. It is assumed that the wall above its intersection with the curved failure surface is acted on by a normal stress that can be approximated by $\sigma_o K_A$. The length of wall affected is given by $(B/2)\tan(45+\phi/2)$ plus y. For $\phi = 35°$ the value of $(B/2)\tan(45+\phi/2)$ is $1.92(B/2)$. A reasonable assumption for the loaded wall height would be a value somewhat greater than this, say 1.2B. The total vertical load resisted by wall friction is $\sigma_4 \times \frac{B^2}{4}$; i.e., the vertical force $B^2\sigma_4$ is carried by four cell walls.

Therefore

$$(\sigma_1 + \sigma_2 + \sigma_3 + \sigma_4)K_A \times \tan\delta \times 1.2B \times B = \sigma_4 \times \frac{B^2}{4} \qquad (23)$$

For the example $\sigma_1 + \sigma_2 + \sigma_3 = 27.2 + 3.1 + 0 = 30.3$, and $\tan\delta$, the friction between sand and cell wall, is taken as 0.3. Thus

$$(30.3 + \sigma_4)0.3 \times 0.3 \times 1.2 = \sigma_4/4$$

$$\sigma_4 = 23.1 \text{ psi}$$

with these values

$$\sigma_o = \sigma_1 + \sigma_2 + \sigma_3 + \sigma_4 = 53.1 \text{ psi}$$

as opposed to 72.2 psi measured in the test. Thus agreement is better using this approach, but it is still not too good. As experiments indicate, however, that cell bursting is extremely unlikely for any case where the loaded area does not fall entirely within the plan area of a single cell, more refined analyses are not considered warranted at

17

this time.  Instead it is suggested that cell dimensions be chosen to insure that the loaded area always includes at least one joint beneath it regardless of position if possible.

## BEARING CAPACITY ANALYSIS

Sand-filled grid cells overlying a soft subgrade represent a two layer system for which no rigorous and correct bearing capacity solution appears to exist.  If it is assumed, however, that the allowable loading is controlled by the soft subgrade, then a suitable approach may be to (1) limit the vertical stress in the subgrade to a value less than its bearing capacity and (2) limit the maximum shear stress in the subgrade to a value less than the subgrade shear strength.

Estimates of the maximum vertical and shear stresses in the subgrade could be made using two-layer elastic theory or by finite element analysis if values for the modulus of the subgrade and for the grid cell layer could be obtained.  A reasonable estimate of the modulus of the subgrade can be made if its CBR or modulus of subgrade reaction are known.  Unfortunately, simple analytical estimation of the modulus of grid cells does not seem possible because of the stress-dependent nature of the sand stiffness and the three-dimensionality of a grid cell network.  Accordingly, a series of simple model tests has been done to evaluate the equivalent elastic moduli for different sizes of loaded areas, grid cell widths, and heights.  These tests and their results are described in a subsequent section of this report.

BENDING FAILURE

An analysis of bending deflections and the potential for tensile failure at the bottom of the grid cell layer could be made if an effective modulus could be obtained for the layer. As for the bearing capacity evaluation discussed in the last section, such a determination has not been possible. Easily applied axisymmetric and two-dimensional finite element computer programs are available; however, neither of these conditions can model the grid cell geometry and properties even approximately. Consideration has been given to the possible application of three-dimensional finite element programs; however, none appears available that could be applied within reasonable bounds of cost and computer capacity. Thus, experimentally measured values indicating the influences of grid dimensions and sand properties on layer modulus seems the only suitable approach.

For any case in which loading conditions, subgrade characteristics, and deflections are known, an equivalent modulus can be calculated for the grid cell layer. This can, in turn be used to compute the maximum tensile stress to be carried by the grid cell material on the basis that the sand fill cannot carry tension.

ANALYSIS OF RUTTING

The difficulties in prediction of rut development were noted earlier. It was suggested that an approach to limiting the development of large permanent deformations would be to limit both stresses in the subgrade and resilient deformations. Increasing the stiffness or modulus of the grid cell layer would reduce these stresses and deformations. Some correlation

19

between the observed rut depths in the tests described by Webster and Alford (1978) and estimated modulus values for the reinforced layers has been obtained and is presented later in this report.

## GRID CELL MODEL TESTS

A series of model tests were done to obtain additional information on the reinforcing effect of grid cells. In particular it was desired to obtain a better understanding of the influences of cell dimensions on stiffness and bearing capacity of the reinforced sand layers. Specific variables studied were a/h, the ratio of radius of loaded circular area to cell height, and a/B, the ratio of loaded area radius to cell width.

The apparatus and procedures used for these tests were the same as described by Rea and Mitchell (1978), except that the grid cell reinforced sand layer was placed directly on a concrete floor rather than a spring base. With this arrangement it was possible to back calculate an equivalent elastic modulus for the reinforced layer using elastic theory solutions developed for homogeneous elastic layers overlying a rigid base.

### Apparatus and Procedure

The tests were done in a box 36 inches (0.915m) square. A uniform, fine quartz sand (Monterey No. 0) having a mean particle size of 0.36 mm and a coefficient of uniformity of 1.45 was used. In all tests the sand was vibrated to its maximum density of 107 lb/ft$^3$ (1,710 kg/m$^3$). After filling the grid cells the sand was levelled at the top of the cell walls. With the exception of one test, no stress-distributing cover layer was used above the cells.

20

Circular loading plates of various sizes were used. All tests were of the "O" type, i.e., the center of the loading plate was placed directly over the center of a grid cell. In the study reported by Rea and Mitchell (1978), "X" tests were also done, wherein the loading plate was centered over the intersection between two cells.

All tests were done using paper cells which were square in plan and had a width B of 2 inches. By varying the diameter of loading plate 2a and the cell height h, it was possible to investigate a range of a/h and a/B values. The paper cell wall thickness was 0.008 in. (0.2 mm).

Only static load tests were done, and values of bearing capacity and modulus were computed using the deformations measured on first loading. Modulus values were based on the initial straight line portions of the load-settlement curves.

One-dimensional compression tests were also done on both reinforced and unreinforced sand samples. The results of these tests can be assumed to give modulus values corresponding to a/h = ∞. Finally, a test was done using a 1.5 in (38 mm) thick layer of coarser sand (Monterey No. 20) over a 6 in. (150 mm) thick reinforced layer to evaluate the effect of a cover layer on modulus.

## Test Results

The results of the test program are shown in Figs. 9 to 16 in the form of footing stress vs. vertical settlement of the loading plate. The results of the main test program are summarized in Table 1. where the bearing capacity and equivalent elastic modulus E are also given. As noted previously, the values of E were computed using available elastic solutions (e.g., Poulos and Davis, 1974) for the settlement of a circular loaded area

21

# TABLE 1

## SUMMARY OF PAPER GRID CELL MODEL TEST RESULTS

| Test No. | Thickness h (in.) | Plate Radius a (in.) | Rein. (R) Unrein. (U) | a/h | a/B | h/B | Bearing Capacity (psi) | Modulus (psi) |
|---|---|---|---|---|---|---|---|---|
| 1 | 2 | 0.625 | U | 0.312 | - | - | 10 | 87 |
| 2 | 2 | 1.500 | U | 0.750 | - | - | 23 | 390 |
| 3 | 2 | 3.00 | U | 1.500 | - | - | 41 | 570 |
| 4 | 2 | 1.000 | R | 0.500 | 0.500 | 1.0 | 74 | 335 |
| 5 | 2 | 1.500 | R | 0.750 | 0.750 | 1.0 | 76 | 878 |
| 6 | 2 | 3.000 | R | 1.500 | 1.500 | 1.0 | * | 950 |
| 7 | 4 | 0.625 | U | 0.156 | - | - | 9 | 92 |
| 8 | 4 | 1.500 | U | 0.375 | - | - | 23 | 238 |
| 9 | 4 | 3.000 | U | 0.750 | - | - | 27 | 433 |
| 10 | 4 | 0.625 | R | 0.156 | 0.312 | 2.0 | 64 | 308 |
| 10a | 4 | 0.625 | R | 0.156 | 0.312 | 2.0 | 76 | 520 |
| 11 | 4 | 1.500 | R | 0.375 | 0.750 | 2.0 | 108 | 663 |
| 11a | 4 | 1.500 | R | 0.375 | 0.750 | 2.0 | 118 | 890 |
| 12 | 4 | 3.000 | R | 0.750 | 1.500 | 2.0 | * | 673 |
| 12a | 4 | 3.000 | R | 0.750 | 1.500 | 2.0 | * | 910 |
| 13 | 6 | 0.625 | U | 0.104 | - | - | 9 | 77 |
| 14 | 6 | 1.500 | U | 0.250 | - | - | 20 | 191 |
| 15 | 6 | 3.000 | U | 0.500 | - | - | 26 | 336 |
| 16 | 6 | 0.625 | R | 0.104 | 0.312 | 3.0 | 78 | 502 |
| 17 | 6 | 1.500 | R | 0.250 | 0.750 | 3.0 | 105 | 1090 |
| 18 | 6 | 3.000 | R | 0.500 | 1.500 | 3.0 | * | 1257 |
| 19 | 6 | 2.500 | R | 0.417 | 1.25 | 3.0 | * | 1540 |
| 20 | 6 | 2.500 | R | 0.333 | 1.25 | 3.5 | 75 | 1530 |

*Bearing capacity exceeded apparatus loading capacity.

on an elastic layer of finite thickness over a rigid base. A value of Poisson's ratio of 0.35 was assumed for these calculations. For those tests where no bearing capacity is indicated in Table 1 (No. 6, 12, 12a, 18, 19,), the bearing capacity exceeded the capacity of the loading frame.

It may be seen from Figs. 9 to 16 that the initial portions of the load-settlement curves were nearly linear in most cases, thus providing a basis for estimation of an effective layer modulus applicable for a reasonable loading range. In most cases failure was by bursting or tearing of cells for tests in which the diameter of the loading plate was less than the width of cell. For tests in which the plate was large enough in diameter to extend over joints connecting adjacent cells, failure generally involved buckling of joints. Examples of these failure modes are shown in Figs. 17 and 18.

Values of constrained modulus were calculated from the results of one-dimensional compression tests on unreinforced and reinforced samples 2-in. high as indicated in Table 2. Equivalent Young's modulus values were calculated using elastic theory and an assumed value of Poisson's ratio of 0.35.

The results of the test to evaluate the influence of the cover layer of coarser sand are given in Table 3. The equivalent modulus for the test in which a 1.5 in. thick cover layer was used was computed assuming a composite layer of 7.5 in. thickness. The bearing capacity of the system without a cover layer was greater than the capacity of the loading system; whereas, that in the test with a cover layer was 75 psi. Failure in the system with a cover layer was in the form of joint buckling and rupturing accompanied by penetration of some of the cover layer sand into the lower

## TABLE 2

### ELASTIC MODULUS VALUES FOR ONE-DIMENSIONAL LOAD TESTS

#### Test Results

| Load (kg) | Stress (psi) | Reinforced | | Unreinforced | |
|---|---|---|---|---|---|
| | | Deflection $(10^{-3}$ in.$)$ | Axial Strain % | Deflection $(10^{-3}$ in.$)$ | Axial Strain % |
| 10 | 0.85 | 0.5 | 0.025 | 5 | 0.25 |
| 20 | 1.69 | 1.5 | 0.075 | 9 | 0.45 |
| 30 | 2.54 | 2.5 | 0.125 | 12 | 0.6 |
| 40 | 3.39 | 3.5 | 0.175 | | |
| 50 | 4.23 | 4.0 | 0.200 | | |

Cell height, h = 2 in.     Footing Radius, a = 2.88 in.

#### Modulus Calculations

| | Load Increment | Vertical Stress Increment, $\Delta\sigma_v$ (psi) | Vertical Strain Increment, $\Delta\epsilon_v$ (%) | Constrained Modulus $M_v$ (psi) | Young's Modulus E (psi) |
|---|---|---|---|---|---|
| Unreinforced | 0-20 kgs | 1.69 | 0.45 | 376 | 234 |
| | 0-30 kgs | 2.54 | 0.60 | 423 | 264 |
| | 10-30 kgs | 1.69 | 0.35 | 483 | 301 |
| Reinforced | 0-20 | 1.69 | 0.075 | 2253 | 1404 |
| | 0-50 | 4.23 | 0.200 | 2115 | 1322 |
| | 10-30 | 1.69 | 0.100 | 1690 | 1056 |
| | 10-50 | 3.38 | 0.175 | 1931 | 1207 |
| | 20-50 | 2.54 | 0.125 | 2032 | 1266 |

$$m_v = \frac{\Delta\sigma_v}{\Delta\epsilon_v} \; ; \quad E = m_v \frac{(1+\mu)(1-2\mu)}{(1-\mu)} \; ; \quad \mu = 0.35 \; \rightarrow \; E = \frac{m_v}{1.605}$$

# TABLE 3

## EFFECT OF COARSER SAND COVER LAYER

Cell height = 6 in.        No.  0 Monterey Sand Cell Fill

Cell width  = 2 in.        No. 20 Monterey Sand Cover Layer

| | Bearing Capacity (psi) | Modulus (psi) |
|---|---|---|
| Without Cover Layer | >80 | 1540 |
| With Cover Layer | 75 | 1530 |

layer. Some local buckling was observed 2 in. below the surface in the system without a cover layer.

These test results would suggest that the use of a cover layer offers little improvement. It is known, however, from the results of field tests under traffic and the repeated load tests of Rea and Mitchell (1978) that without a protective layer over the tops of the grid cells, sand is readily displaced, the cell walls become subjected to direct vertical loads, and cell failure soon develops.* It seems, therefore, that the beneficial influence of a cover layer is to protect the reinforced layer, not in strength and modulus improvement.

## Analysis of Test Results

Figure 19 shows bearing capacity of the sand, both with and without reinforcement, as a function of the ratio of load plate radius to layer thickness a/h. The results show that irrespective of the value of a/h the grid reinforced sand layer had a higher bearing capacity than the unreinforced sand. The improvement increased with increasing thickness of reinforced layer (h/B), although it appears that increasing h/B beyond 3.0 might not result in significant further improvement.

It must be remembered, however, that the data shown in Fig. 19 pertain to sand layers overlying a rigid base. Were there a soft subgrade, the bearing capacity of the two layer system could be expected to increase until the failure zone were contained totally within the sand.

That the bearing capacity of the unreinforced sand layer increased regularly with increase in radius of loaded area is consistent with the usual behavior of sands. Increased size of loaded area means increased confinement, and increased confinement results in increased strength.

---

*S. L. Webster (personal communication, 24 Oct. 1978) reported that penetration asphalt treatment of the surface of the sand in grid cells has given good performance under traffic without the use of a cover layer.

The substantial increase in bearing capacity and protection afforded
to soft subgrades provided by granular surface layers has been discussed
by Mitchell and Gardner (1971). Additional protection that could be given
by grid cell reinforcement of the sand is suggested by the results in
Fig. 19. The results of these tests and also the results of the tests
reported in Fig. 12 of Rea and Mitchell (1978), reproduced here as Fig. 20,
support the conclusion that a ratio of cell height to width h/B of
2 to 3 should be an optimum.

The variation in Young's modulus with a/h for unreinforced and
reinforced sand layers of different thickness is shown in Fig. 21. For
unreinforced sand the modulus is essentially independent of layer thickness.
It increases with plate size as would be expected, because of the greater
confinement. The modulus corresponding to an infinite width of loaded
area (one-dimensional case) is seen to be less than that for inter-
mediate values of a/h for the unreinforced sand. No ready explanation for
this result is available.

The results in Fig. 21 indicate a several fold increase in modulus
when grid cell reinforcing is used. The improvement increases with increasing
h/B and appears to be an optimum for values of a/B of the order of 1.0.
Although the available apparatus did not enable testing over a sufficiently
wide range of a/h to establish the full shapes of the modulus curves, it
does appear that the modulus values pass through maxima and minima with
increasing a/h values. Fig. 21 shows also that for very large values of a/h
a common value of E should be obtained for a given value of cell size (B) and
all values of h. This would be expected, because large values of a/h
correspond to essentially one-dimensional loading.

Figure 10 of Rea and Mitchell (1978) indicates also that the bearing capacity of grid reinforced sand layers over a soft subgrade ($k$ = 50 psi/in) passes through maxima and minima for increasing sizes of loaded area. These data have been replotted here as Fig. 22 in terms of bearing capacity as a function of $a/h$ for different values of $h/B$. Again the tendency for peaks and valleys can be seen.

Equivalent elastic moduli values have been computed for Rea and Mitchell's test data using the Westergaard equation for an elastic layer over a Winkler foundation. The modulus of subgrade reaction for these tests, $k$, was 50 psi/in., and Poisson's ratio was assumed to be 0.35. Corresponding stresses and deflections for the analysis were taken from the straight line portions of the load-settlement curves. These values, as well as corresponding values of bearing capacity, are shown in Fig. 23. In Rea and Mitchell's investigation tests were done with the loading plate centered both over the center of grid cells ("0" tests) and over grid cell inter-sections ("X" tests). The values shown in Fig. 23 correspond to the test type giving the smallest values of bearing capacity and modulus.

The values of modulus obtained from Rea and Mitchell's data are significantly less than those obtained in the present study where the grid cell layer was underlain by a rigid base. This indicates the dependence of the reinforced layer stiffness on the modulus of the underlying layer, a finding consistent with previous observations of the variations of the modulus of granular bases with subgrade modulus.

Although the irregular curve shapes in Figs. 21-23 may appear some-what surprising, it is believed that their explanation lies in the number of grid cell joints underlying the loaded area. These joints exert a

28

definite stiffening effect on the system, and the greater the number of joints per unit area of loading plate, the greater the bearing capacity and modulus values.

The relationship between plate size and number of joints per unit area for 2-inch grid cells can be seen in Fig. 24 for "O" tests, and in Fig. 25 for "X" tests. It may be seen from these figures that the number of joints per unit area varies significantly for different plate sizes. It may also be seen that a slight misalignment in placement of the load plate over grid cells in a test program could result in significantly different numbers of joints and lengths of cell walls being overlain by the loading plate. For example, for the "O" test condition shown in Fig. 24, a slight misalignment of the 3-inch diameter load plate could result in the loading of only three joints instead of four, and misalignment of the 6-inch diameter plate would lead to incorporation of two extra joints. Because the test arrangement was such that small misalignments between the center of the loading plate and the center of a grid cell could not be avoided, this may explain the apparent scatter in the results shown in Fig. 21 for the tests on a 4-inch thick layer corresponding to a 3-inch diameter plate $(a/h = 0.75)$.

A heavy dashed line is shown on Fig. 23 which indicates the number of joints per square inch of loading plate area as a function of a/B. The values shown are for either "O" or "X" loading, whichever gives the least value, as the indicated values of bearing capacity and modulus also correspond to the most critical loading conditions. The comparison shows reasonable consistency between the number of joints per unit area and the values of modulus and bearing capacity. A much more extensive test program would be required, involving many more values of a/B, to establish a conclusive correlation, however.

29

The modulus values obtained in the present study and listed in Table 1 have been replotted in Fig. 26 as a function of a/B. Also shown by a heavy dashed line is the relationship between number of joints per unit area and a/B for the "O" loading conditions used for these tests. The number of tests is far too few and the number of variables is too great to allow the establishment of exact correlations. The data do not exclude the possibility, however, that for a given value of h/B the relationship between modulus and a/B would be of the same form as that between number of joints per unit area and a/B.

## Conclusions from the Model Test Program

The results of the model test programs done as a part of this investigation and by Rea and Mitchell (1978) lead to the following conclusions:

1. The load-settlement behavior of plates on grid cell reinforced sand layers is approximately linear up to moderate stress levels.

2. Failure generally involved cell bursting or tearing for cases where the plate diameter was less than the cell width and buckling of joints for those cases where the plate extended over the joints connecting cells. It should be noted that the experimental arrangements were such that penetration of cells into a soft subgrade was not possible.

3. The use of a coarser grained cover layer over the sand-filled grid cells did not give improved bearing capacity or modulus. Repeated load tests and field traffic tests have shown, however, that cover layers or surface sealing are essential to provide containment for the sand in

the cells and to prevent direct vertical load application to the cell walls.

4. In general bearing capacity increases with size of loaded area and thickness of grid cell layer. The optimum ratio of cell height to width h/B is of the order of 2 to 3.

5. Grid cell reinforcement can lead to a several fold increase in the effective modulus of a sand layer. This increase increases with h/B and appears to be an optimum for a/B in the range of about 1.0.

6. The modulus of the reinforced sand depends on the subgrade modulus.

7. Bearing capacity and modulus vary irregularly with a/h and a/B for the systems tested. Although some of the variation can be ascribed to experimental error, the principal factor appears to be related to the number of cell joints per unit area of loading plate. If a minimum cell size is chosen so that a/B > 0.7 for square cells (in plan), then there will always be at least one joint under the loaded area regardless of its position. In addition the possibility of cell failure by bursting will be minimized.

### RUT DEPTH - MODULUS RELATIONSHIP

It was noted earlier that prediction of permanent deformations in pavements is a most complex problem. It was suggested, however, that a suitable approach to minimizing rutting in a given case could be to limit the compressive and shear stresses in the subgrade. This, in turn, can be accomplished by increasing the thickness and modulus of the surface layer. To test the potential of this approach the results of the model tests done in this

31

investigation to evaluate some effects of grid cell geometries have been combined with the results of the Corps of Engineers field tests at WES reported by Webster and Alford (1978).

Characteristics of the WES test sections are given in Table 4. All sections were constructed over a subgrade having a CBR of 0.9 to 1.4. A two to three inch thick gravel surface layer was used over the grid cells. Loaded area radius was taken as 6 inches for these analyses, which is reasonable for the wheel loads and tire pressures used.

Relative modulus values for the reinforced and unreinforced layers, $E_r$ and $E_u$ have been listed in Table 4. These were obtained from the paper grid cell model test results in Fig. 21 and can be considered only as relative values that may reflect the influences of cell geometry and size of loaded area. Actual equivalent modulus values for the field sections are not available. The ratio $E_r/E_u$ is considered to be a measure of the improvement provided by the grid cells.

Deformation values for the test sections as a function of number of coverages are given in Table 5. The ratio of the permanent deformation of the unreinforced section to that of a reinforced section after a given number of coverages can be taken as a measure of the improvement obtained. It has been arbitrarily termed the reinforcement ratio herein. The east track of section 5 was used as the baseline unreinforced section, because the west track was underlain by chicken wire. For all other sections the average of the two deformations recorded in Table 5 was used.

Values of $E_r/E_u$ for the different grid geometries and corresponding values of reinforcement ratio are summarized in Table 6 and plotted in Fig. 27. Although the available data are too few to establish a definitive relationship,

32

## TABLE 4

### WES GRID CELL TEST SECTION DATA

| Test Section | Configuration | $a/h$ | $a/B$ | Relative Modulus of Unreinforced Layer* $E_u$ | Relative Modulus of Reinforced Layer* $E_r$ | $\dfrac{E_r}{E_u}$ |
|---|---|---|---|---|---|---|
| 1 | 6" x 6" x 12" high aluminum cells | 0.5 | 1.0 | 300 | 820 | 2.73 |
| 2 | Same as 1 with T-16 membrane under cells | 0.5 | 1.0 | 300 | 820 | 2.73 |
| 3 | 6" x 6" x 6" high cells over 6" sand layer and T-16 membrane | 1.0 | 1.0 | 460 | 830 | 1.80 |
| 4 | 12" x 12" x 12" aluminum cells over T-16 membrane | 0.5 | 0.5 | 300 | 420 | 1.40 |
| 5 | No grid, 12 inch gravel layer, chicken wire over subgrade in west wheel path | 0.5 | - | 300 | 300 | 1.0 |

33

*From grid cell model test results in Fig. 21.

## TABLE 5

### WES TEST SECTION DEFORMATION DATA

Permanent Deformations - Inches

| Section No.: | 1 | | 2 | | 3 | | 4 | | 5 | |
|---|---|---|---|---|---|---|---|---|---|---|
| No. of Coverages | W* | E* | W | E | W | E | W | E | W | E |
| 10 | – | – | 0.2 | 0.2 | 0.3 | 0.4 | 0.3 | 0.7 | 0.6 | 0.8 |
| 100 | 0.4 | 0.4 | 0.7 | 0.35 | 0.8 | 0.8 | 0.8 | 1.4 | 1.2 | 1.7 |
| 1000 | 1.8 | 1.0 | 1.8 | 1.0 | 6.0 | 1.8 | 2.8 | 4.0 | 2.2 | 4.0 |
| 2000 | 2.8 | 1.75 | 2.2 | 1.3 | | 3.9 | 4.6 | 5.2 | 2.4 | 5.8 |
| 5000 | – | 3.2 | 3.2 | 2.0 | | | | | 2.8 | |
| 10000 | – | | | 6.5 | | | | | 3.0 | |

*W = West tire track

*E = East tire track

34

# TABLE 6

## VALUES OF $E_r/E_u$ AND REINFORCEMENT RATIO FOR WES TEST SECTIONS

| Test Section | No. Coverages | $E_r/E_u$ | Reinforcement Ratio* |
|---|---|---|---|
| 1 | 10 | 2.73 | -- |
| | 100 | 2.73 | 4.25 |
| | 1000 | 2.73 | 2.86 |
| | 2000 | 2.73 | 2.55 |
| 2 | 10 | 2.73 | 4.00 |
| | 100 | 2.73 | 3.24 |
| | 1000 | 2.73 | 2.86 |
| | 2000 | 2.73 | 3.31 |
| 3 | 10 | 1.80 | 2.28 |
| | 100 | 1.80 | 2.25 |
| | 1000 | 1.80 | 1.02 |
| | 2000 | 1.80 | 1.49 |
| 4 | 10 | 1.40 | 1.6 |
| | 100 | 1.40 | 1.54 |
| | 1000 | 1.40 | 1.18 |
| | 2000 | 1.40 | 1.18 |

*Reinforcement Ratio $\equiv$ Deformation of unreinforced section $\div$ deformation of reinforced section.

it does appear that a consistent and reasonable envelope exists which relates the reinforcement ratio to modular ratio. The results show that the greater is the value of $E_r/E_u$ the smaller is the permanent deformation at any number of coverages for the reinforced layer relative to the unreinforced layer. It is seen also that for a given $E_r/E_u$, reinforcement ratio decreases with increasing numbers of coverages.

The consistency of the results supports the use of a/h and a/B as characterizing parameters for grid cell layers. Additional test results would be useful to evaluate the influence of subgrade strength and modulus on behavior, as all the values in Fig. 27 were obtained for test sections on a subgrade of CBR equal to 1.

## CONCLUSIONS

Grid cell reinforced sand layers can provide effective support for traffic over soft subgrades and can provide as much protection as gravel layers up to 1.6 times as thick. This study, aimed at providing an improved understanding of grid cell behavior, with particular reference to failure mechanisms and analytical approaches to design, has led to the following conclusions.

1. Possible grid cell failure modes include (1) cell penetration of the subgrade, (2) cell bursting, (3) cell wall buckling, (4) bearing capacity, (5) bending, (6) durability failure, and (7) excessive rutting.

2. The maximum resistance to penetration of a cell into the subgrade $F_{max}$ is given by

36

$$F_{max} = B^2 \sigma_o \left( e^{4Ktan\delta_m \, h/B} - 1 \right)$$

which shows the importance of cell width B, cell height to width ratio h/B, friction between sand and cell wall $\delta_m$, lateral pressure coefficient of sand K, and vertical stress on the sand in the cell $\sigma_o$.

3. The use of fabric membranes with metal grid cells may be incompatible because cell edges may cut the membrane.

4. The effective modulus of a grid cell reinforced layer may be up to 2 to 3 times that of the unreinforced sand, with the lower value appropriate for h/B = 1 and the higher value for h/B = 3.

5. No simple analysis is possible for evaluation of the bearing capacity or bending resistance of a grid cell reinforced system.

6. Failure by cell bursting is not likely if the diameter of the loaded area 2a is greater than the cell width B; i.e., a/B > 0.5.

7. The main function of a gravel cover layer over grid cells appears to be to protect the cells, not to increase the bearing capacity or modulus.

8. Tests of grid cells over a rigid base suggest an optimum value of h/B for bearing capacity of 2 to 3. This agrees with previous results of Rea and Mitchell (1978) for grid cells over a soft subgrade.

9. Optimum improvement in modulus by the use of grid cells may be for a/B of the order of 1.0.

10. The modulus of a grid cell reinforced layer appears to depend on the modulus of the subgrade.

11. The bearing capacity and modulus appear to depend strongly on the number of grid cell intersections (joints) per unit area of loading plate.

12. If $a/B > 0.7$ for square cells, then there will always be at least one joint under the loaded area regardless of its position. In addition the possibility of cell bursting will be minimized.

13. The ratio of the modulus of a reinforced layer to the modulus of an unreinforced sand layer may be a suitable parameter for prediction of relative rut depths under traffic.

## RECOMMENDATIONS

Available data on grid cell performance are still very limited and many of the hypotheses and conclusions concerning behavior are largely speculative. Accordingly, additional tests and analyses are desirable. Among them would be:

1. Evaluation of the friction coefficient between cell fill and cell wall materials.

2. Measurement of the vertical stress distribution between cell walls and cell fill. This information would be useful to verify the penetration model, to evaluate the stress-distributing effect of the cover layer, and to analyze cell wall buckling behavior.

3. Further study of the possibility for application of finite element methods for analysis of bending and bearing capacity.

4. Development of improved analysis of cell bursting and suitable tests for verification.

5. A carefully designed set of tests to unambiguiously evaluate the dependence of bearing capacity and modulus on the number of joints per unit area.

6. Further tests and analyses to evaluate the usefulness of the reinforcement ratio concept developed herein.

7. Systematic evaluation of $E_r$, the equivalent elastic modulus of the reinforced layer. This parameter is needed for analysis of bending, bearing capacity, and reinforcement ratio. The analyses and tests done thus far show that the following parameters affect the value of $E_r$: $a/h$, the layer geometry ratio; $h/B$, the grid geometry ratio; $a/B$, the loaded area-grid geometry ratio; $E_m$, the modulus of the cell fill material; $E_g$, the modulus of the grid material; $E_s$, the modulus of the subgrade; and $N_j$, the number of grid joints per unit area.

A possible form for the relationship between $E_r$ and these parameters might be

$$E_r = E_u \cdot f_1 \left( \frac{E_g}{E_m} \right) \cdot f_2 \left( \frac{a}{B} \right) \cdot f_3 \, (h/B) \cdot f_4 \left( \frac{a}{h} \right) \cdot f_5 \, (N_j) \cdot f_6 \, (E_s) \qquad (24)$$

where $E_u$ is the modulus of the unreinforced sand layer for the same values of a, h, and $E_s$.

Evaluation of the several functional forms in equation (24) will require an extensive laboratory model test program. Analysis of limiting cases will be helpful to establish upper and lower bounds for some of them.

39

## REFERENCES

Mitchell, James K. and Gardner, William S. (1971) "Analysis of Load-Bearing Fills over Soft Subsoils," Journal of the Soil Mechanics and Foundations Division, ASCE, Vol. 97, No. SM11, Nov. 1971, pp. 1549-1571.

Poulos, H. G. and Davis, E. H. (1974) Elastic Solutions for Soil and Rock Mechanics, John Wiley & Sons, Inc., N.Y., 411 p.

Rea, C. and Mitchell, J. K. (1978) "Sand Reinforcement Using Paper Grid Cells," Preprint 3130, ASCE Spring Convention and Exhibit, Pittsburgh, PA, April 24-28, 1978.

Webster, S. L. and Alford, S. J. (1978) "Investigation of Construction Concepts for Pavements Across Soft Ground," U.S. Army Engineer Waterways Experiment Station, Technical Report S-78- , March 1978.

Webster, S. and Watkins, J. E. (1977) "Investigation of Construction Techniques for Tactical Bridge Approach Roads Across Soft Ground," U.S. Army Engineer Waterways Experiment Station, Technical Report S-77-1.
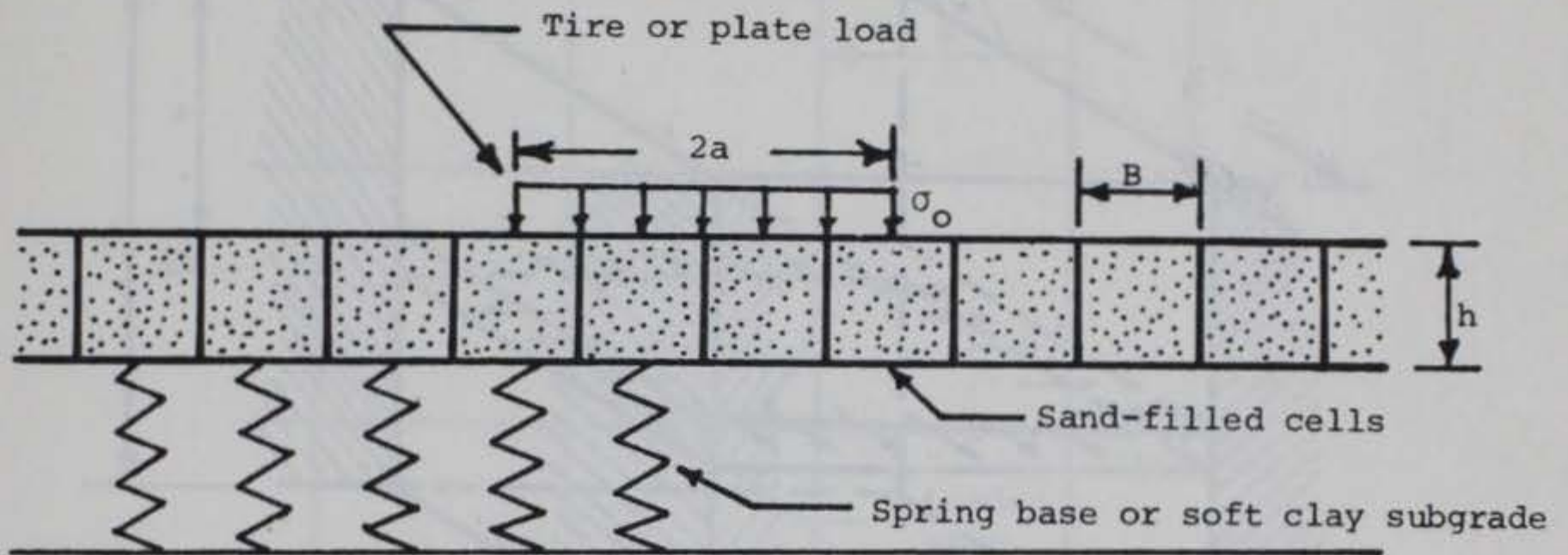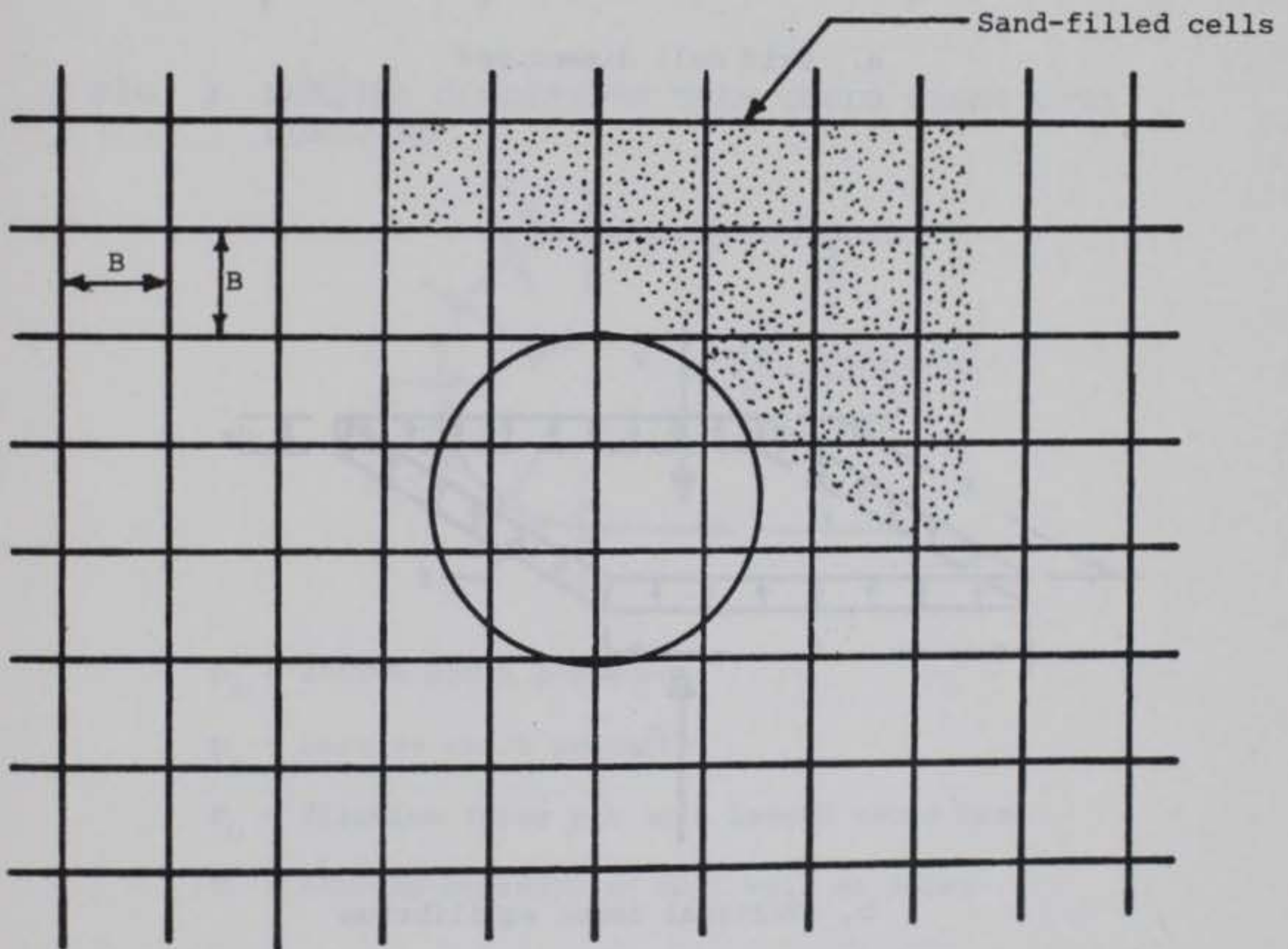
FIG. 1  SCHEMATIC DIAGRAM OF GRID CELL TEST SYSTEMS
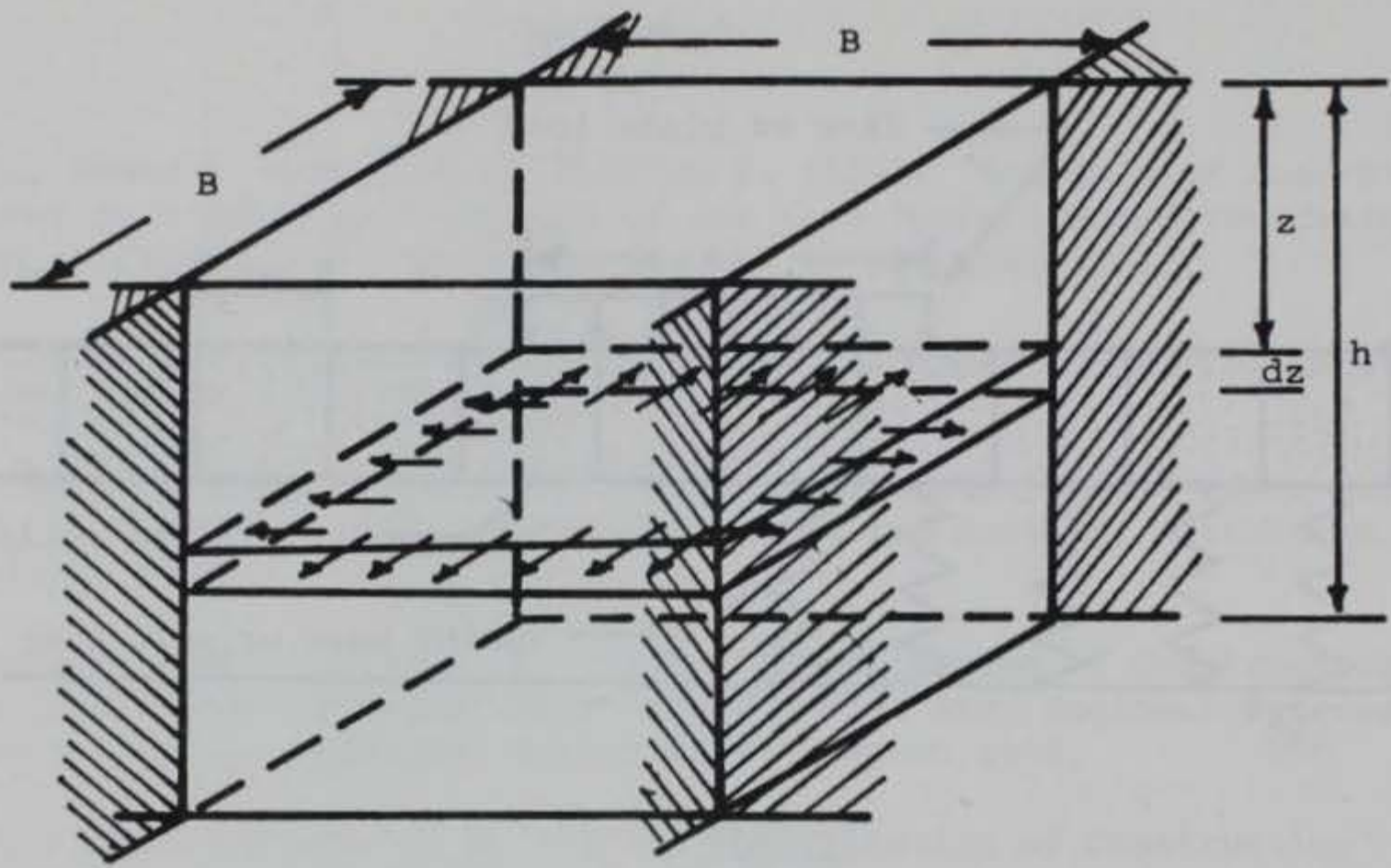
a.  Grid cell dimensions
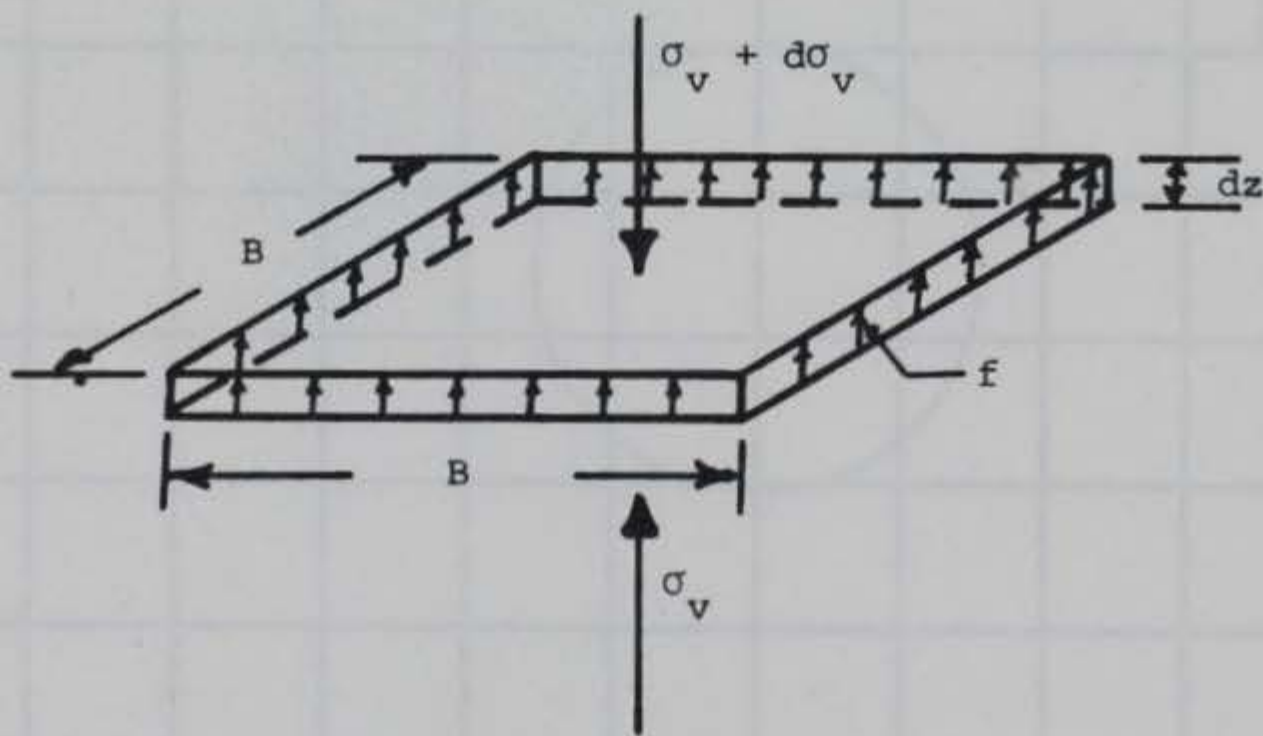


b.  Vertical force equilibrium

FIG. 2   ANALYSIS OF THE PENETRATION RESISTANCE OF A
         SQUARE GRID CELL
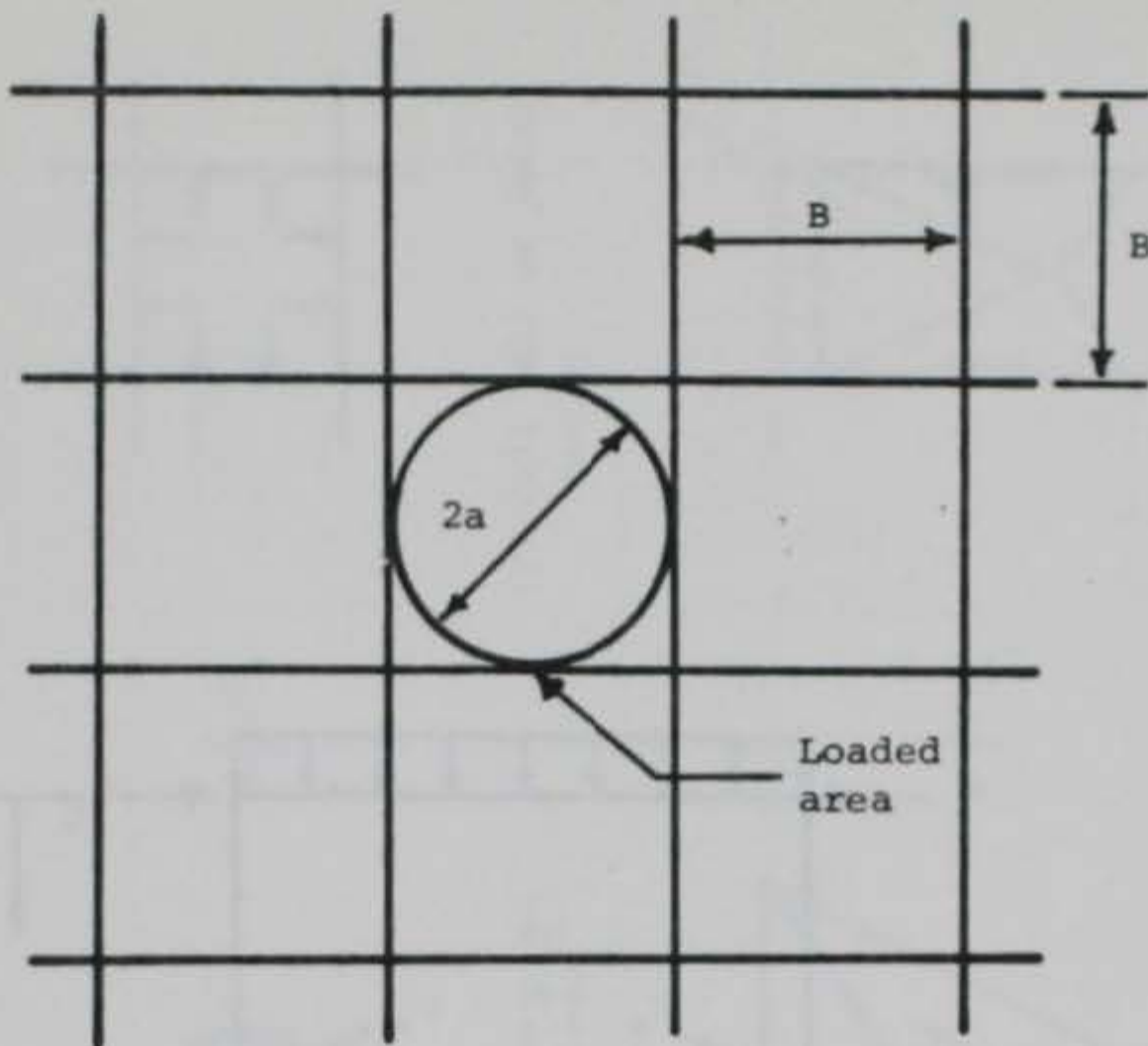
FIG. 3    LOADING CONDITIONS THAT COULD CAUSE CELL
         BURSTING



$$\frac{4B}{\pi} = \frac{\text{Perimeter}}{\pi}$$
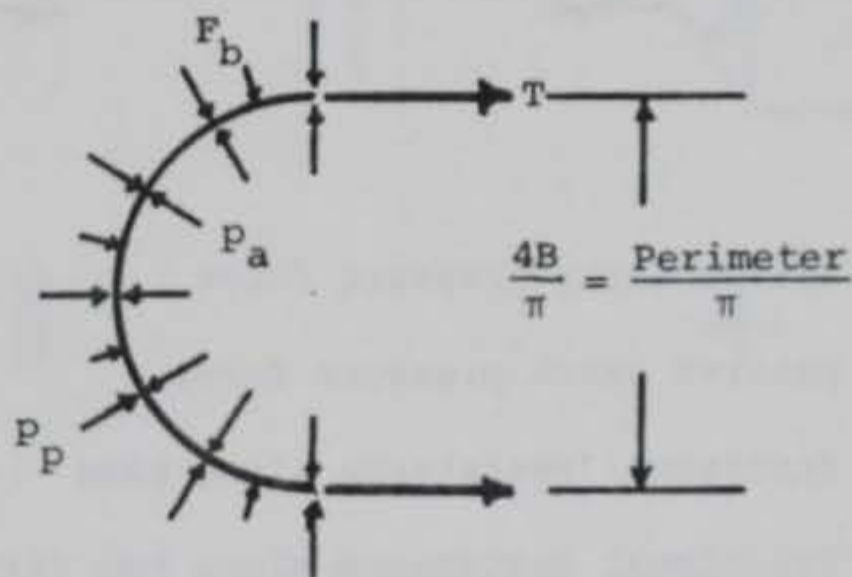
$P_a$ = active earth pressure

$P_p$ = passive earth pressure

$F_b$ = friction force per unit length along base

$T$ = tearing strength of cell wall or joint

FIG. 4    CONDITIONS FOR FAILURE BY CELL BURSTING -
         PLAN VIEW
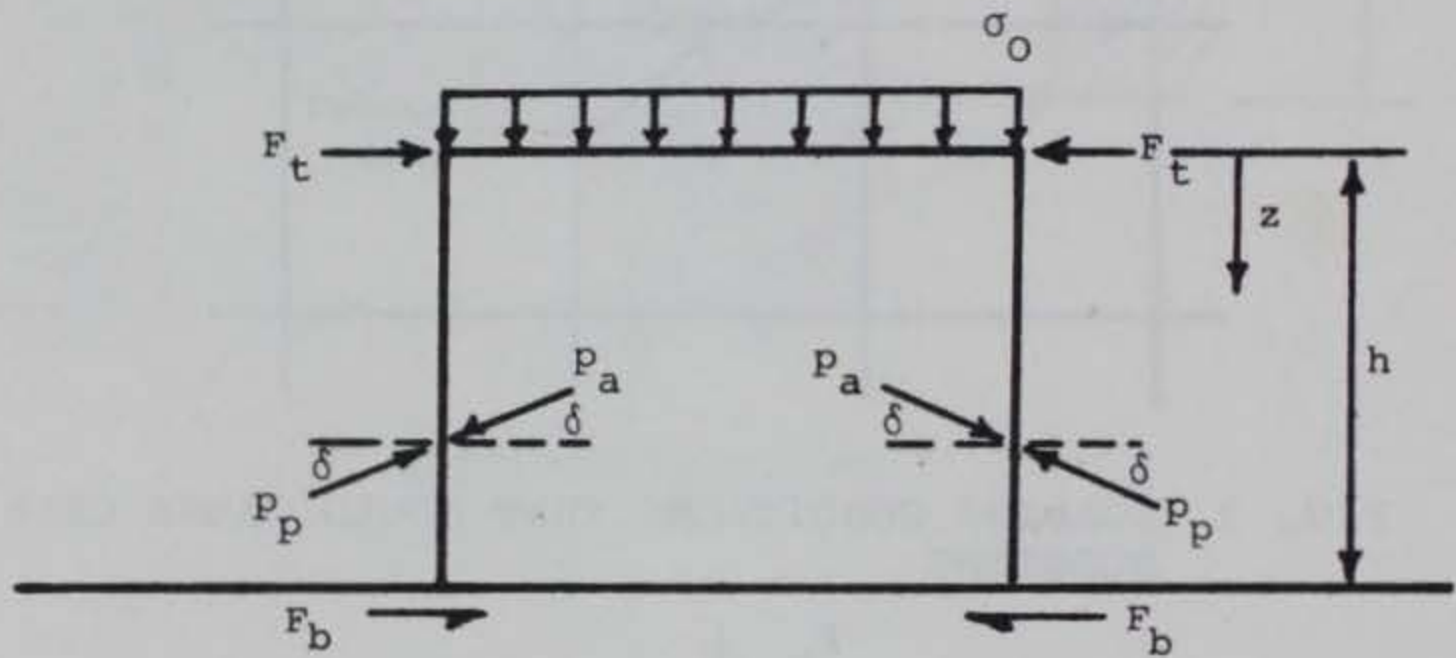
$p_a$ = active earth pressure force

$p_p$ = passive earth pressure force

$F_b$ = frictional resistance along base

$F_t$ = frictional resistance along top (if cover layer present)

$\delta$ = friction angle between sand and cell wall

FIG. 5  CONDITIONS FOR CELL FAILURE BY BURSTING – ELEVATION VIEW

44
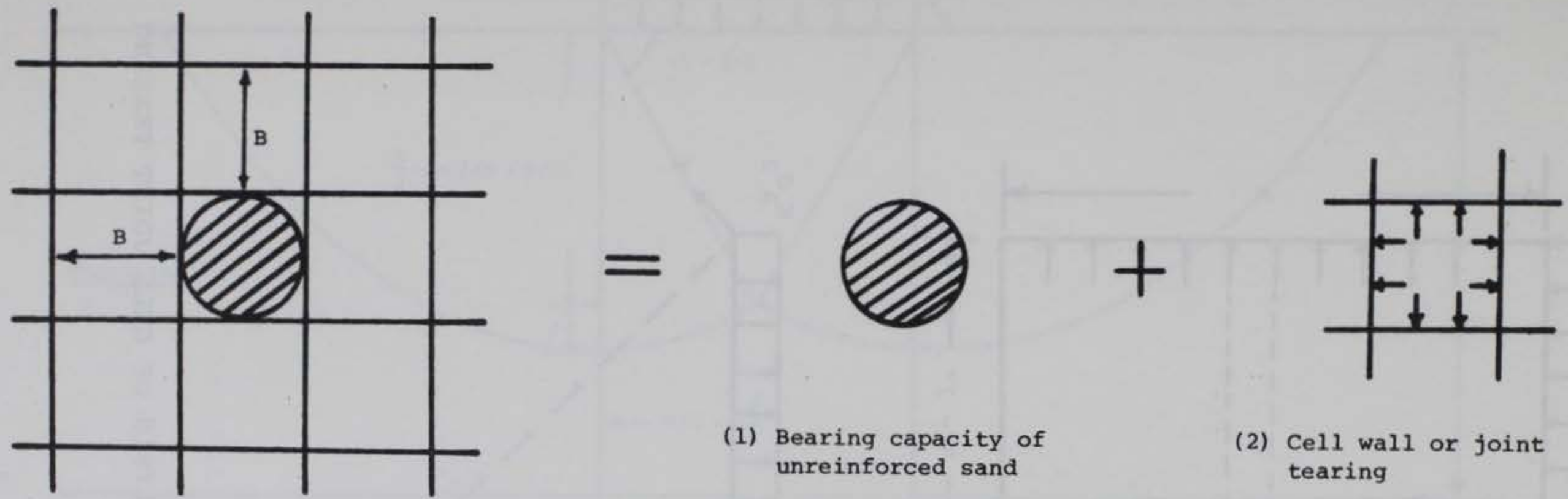
(1) Bearing capacity of
    unreinforced sand

(2) Cell wall or joint
    tearing
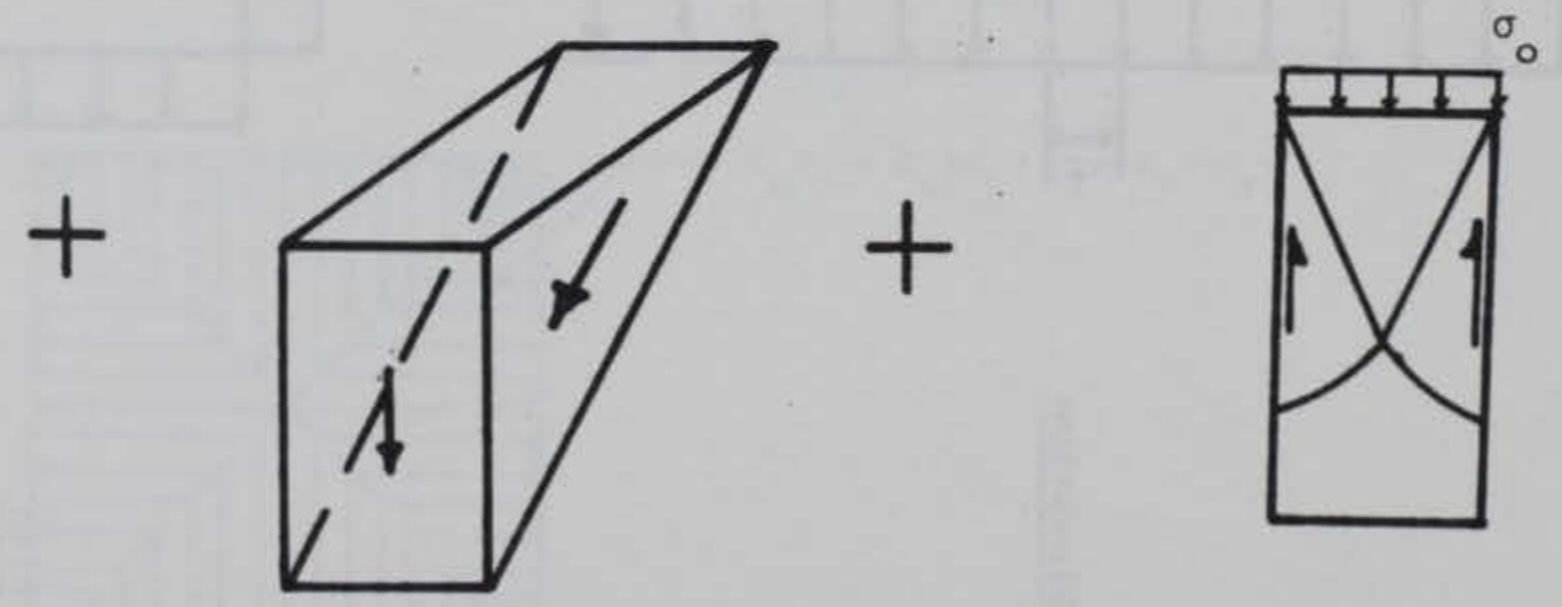
(3) Friction between sand and
    vertical faces in adjacent cells

(4) Side friction along side
    walls of loaded cell

FIG. 6   CONTRIBUTIONS TO CELL
         FAILURE BY BURSTING
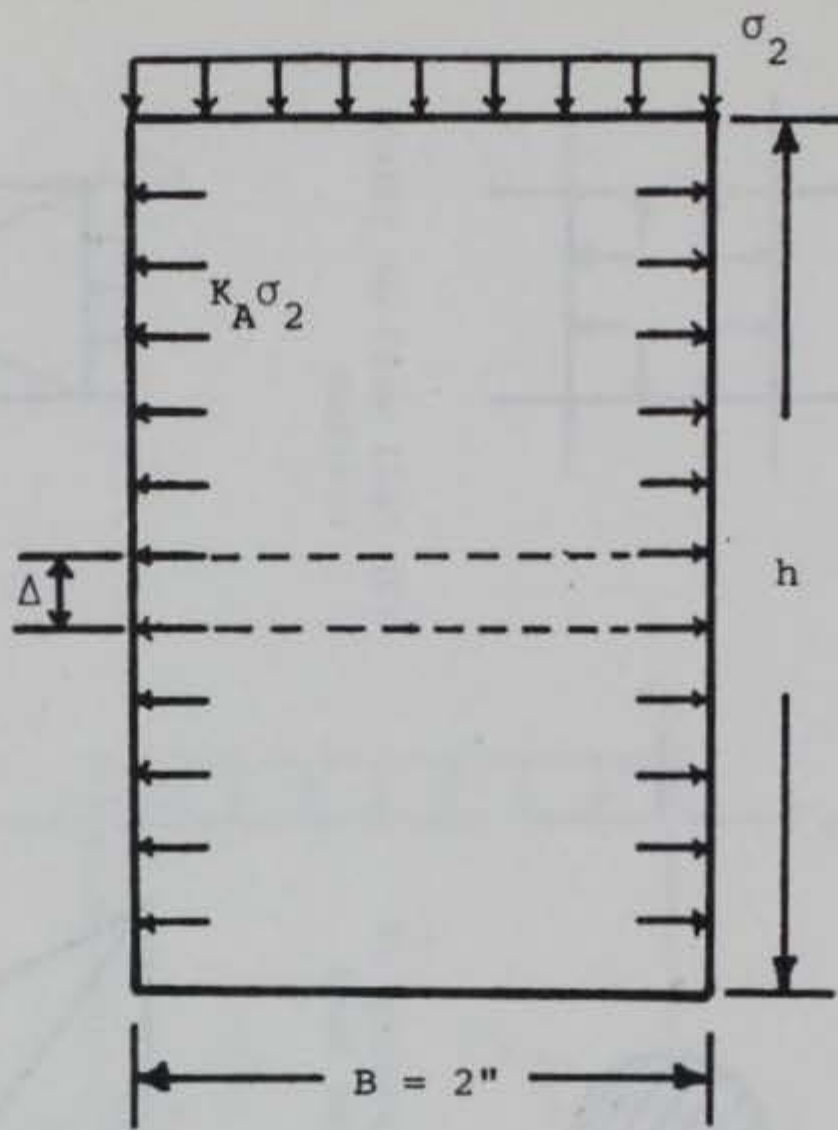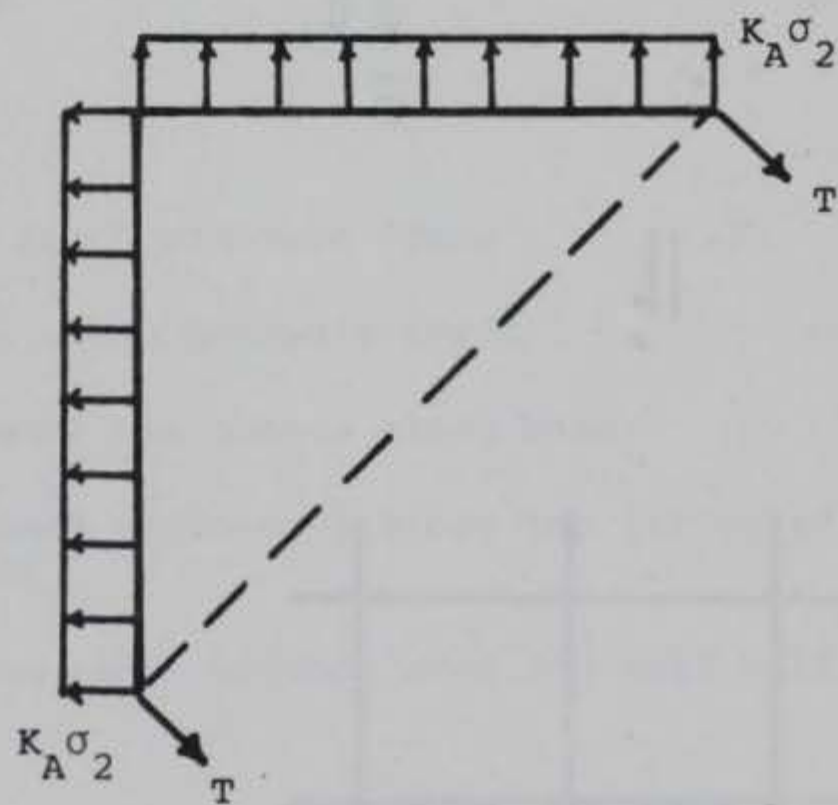
FIG. 7   STRESSES FOR ANALYSIS OF CELL JOINT TEARING

46
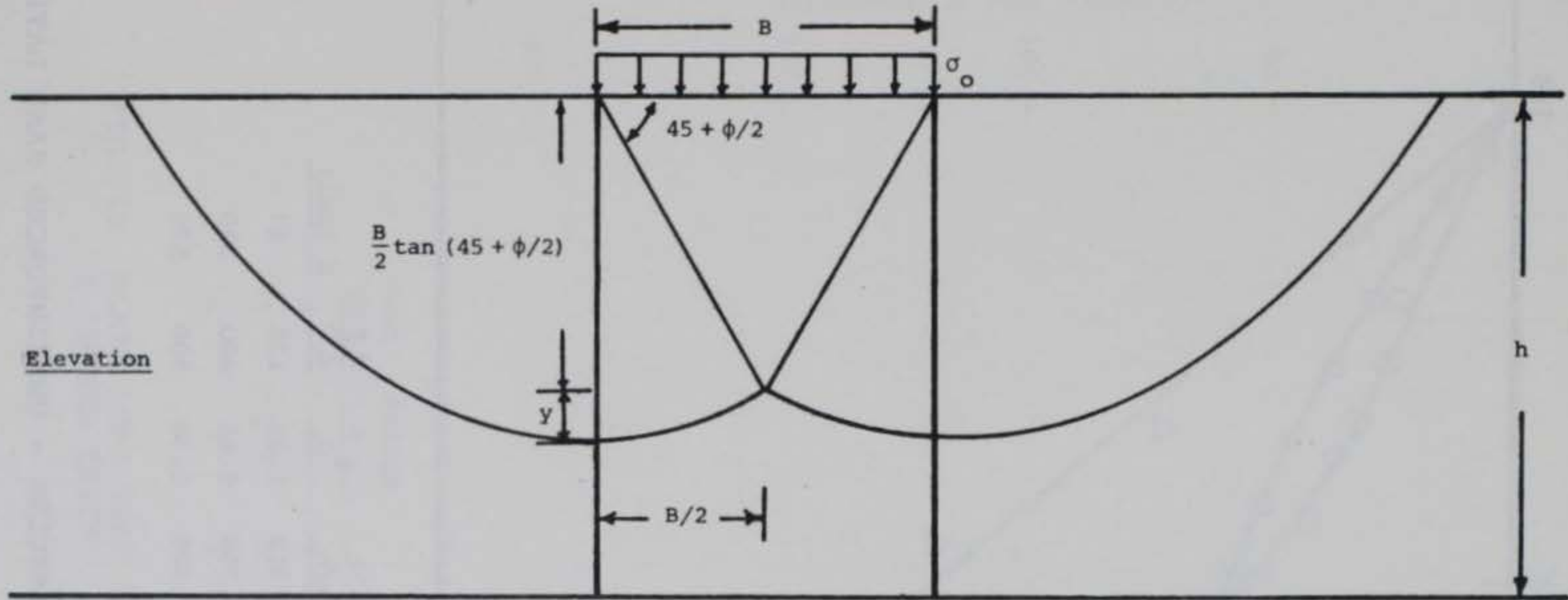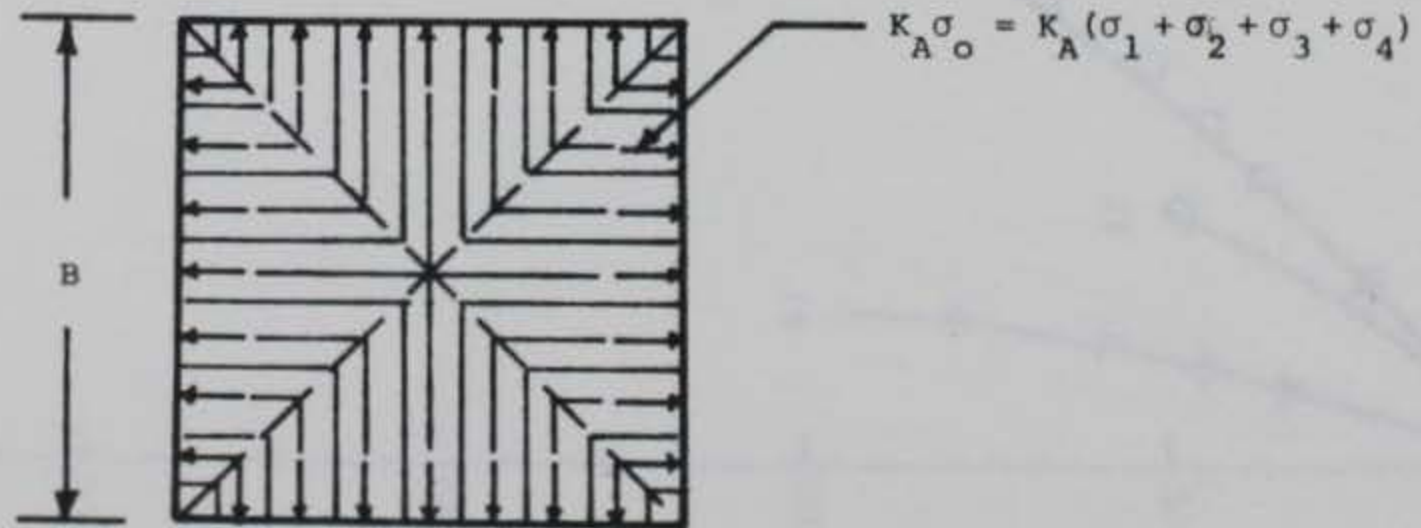
FIG. 8  FAILURE DUE TO DOWNWARD DISPLACEMENT OF SAND WITHIN CELLS

Footing stress (psi)
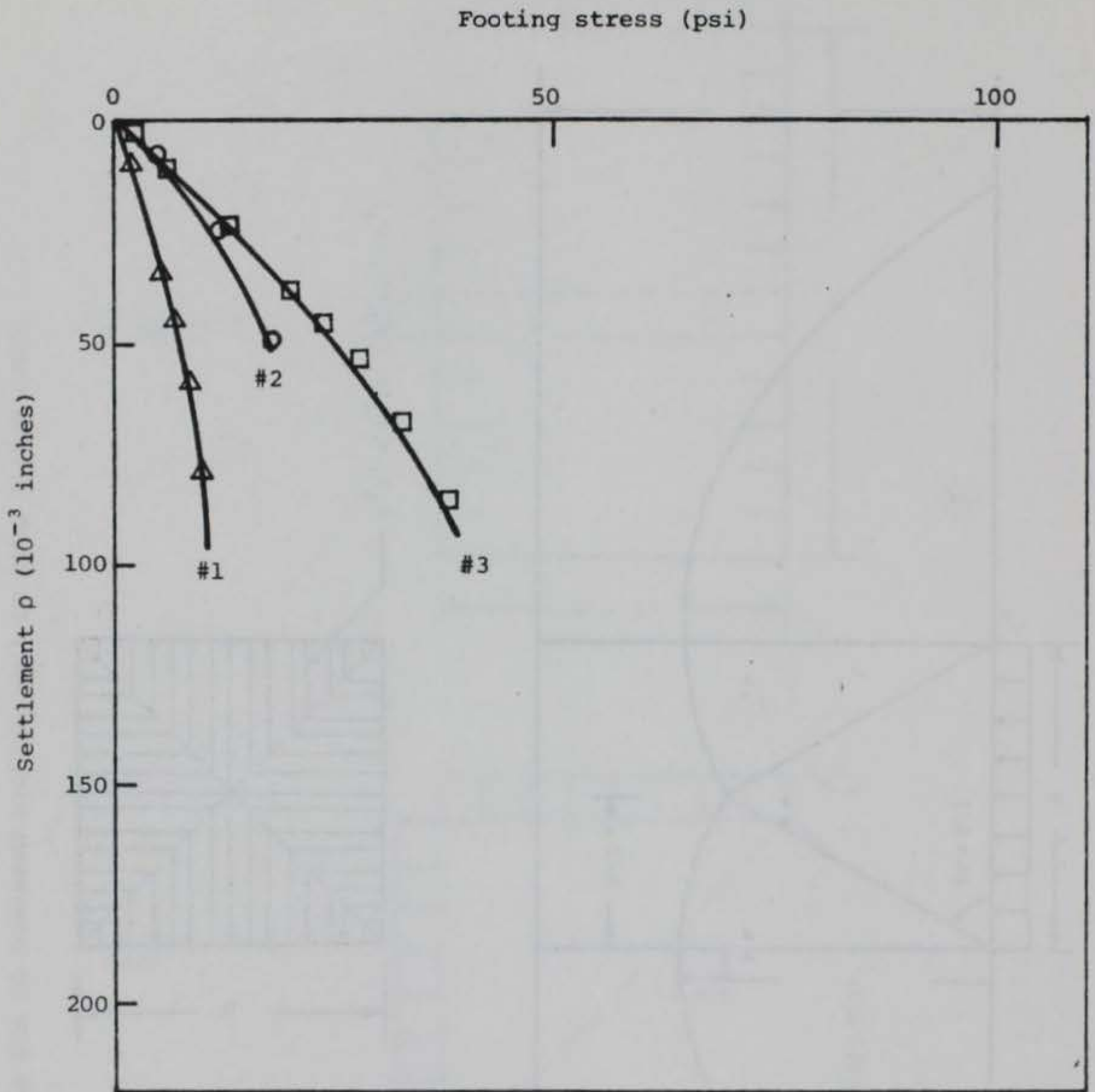


| Test No. | Radius a | a/h | $I_\rho$ | $\frac{\Delta p}{\Delta \rho}$ | E (psi) |
|---|---|---|---|---|---|
| 1 | 0.625 | 0.312 | 1.01 | 135 | 87 |
| 2 | 1.5 | 0.750 | 0.65 | 400 | 390 |
| 3 | 3 | 1.500 | 0.38 | 500 | 570 |

FIG. 9   PLATE LOAD TEST RESULTS - UNREINFORCED SAND LAYER
        2 INCHES THICK

FIG. 10   PLATE LOAD TEST RESULTS - REINFORCED SAND LAYER
2 INCHES THICK
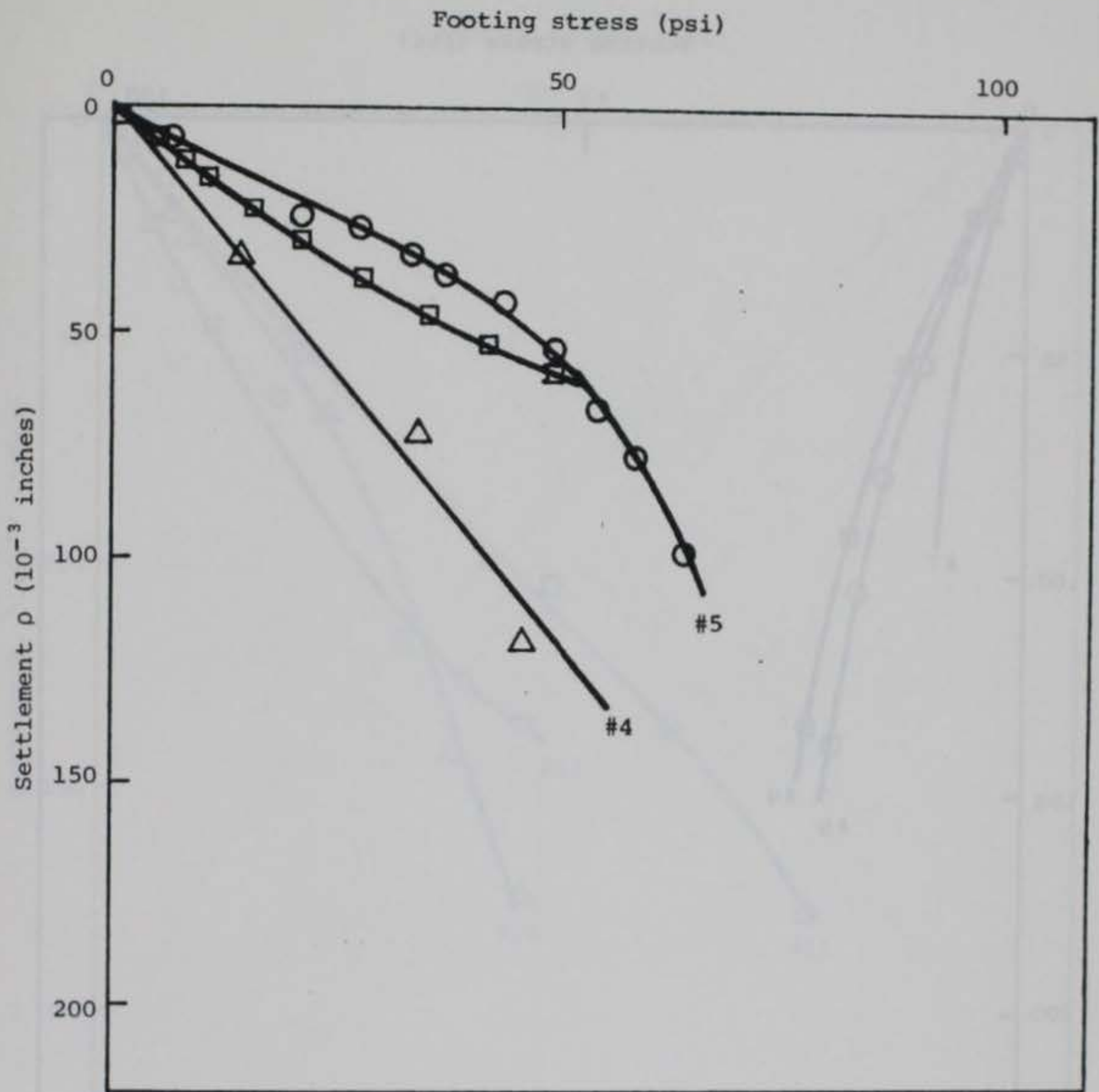
| Test No. | Radius a | a/h | $I_\rho$ | $\frac{\Delta p}{\Delta \rho}$ | E (psi) |
|---|---|---|---|---|---|
| 4 | 1 | 0.500 | 0.82 | 408 | 335 |
| 5 | 1.5 | 0.750 | 0.65 | 900 | 878 |
| 6 | 3 | 1.500 | 0.38 | 833 | 950 |

Footing stress (psi)
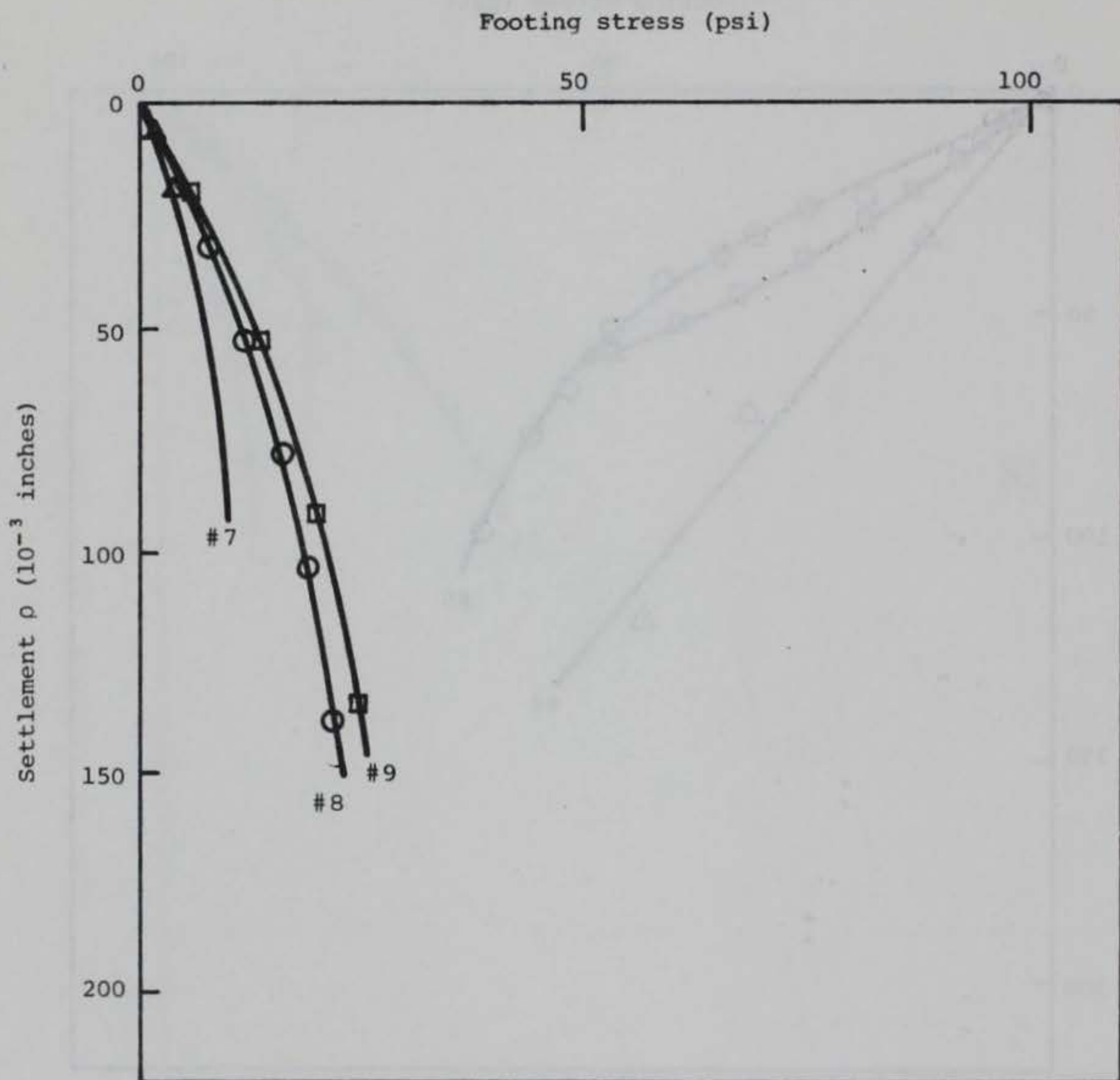


| Test No. | Radius a | a/h | $I_\rho$ | $\frac{\Delta p}{\Delta \rho}$ | E (psi) |
|------|------|------|------|------|------|
| 7 | 0.625 | 0.156 | 1.20 | 123 | 92 |
| 8 | 1.5 | 0.375 | 0.95 | 167 | 238 |
| 9 | 3 | 0.750 | 0.65 | 222 | 433 |

FIG. 11  PLATE LOAD TEST RESULTS - UNREINFORCED SAND LAYER
4 INCHES THICK

Footing stress (psi)

FIG. 12  PLATE LOAD TEST RESULTS - REINFORCED SAND LAYER
4 INCHES THICK
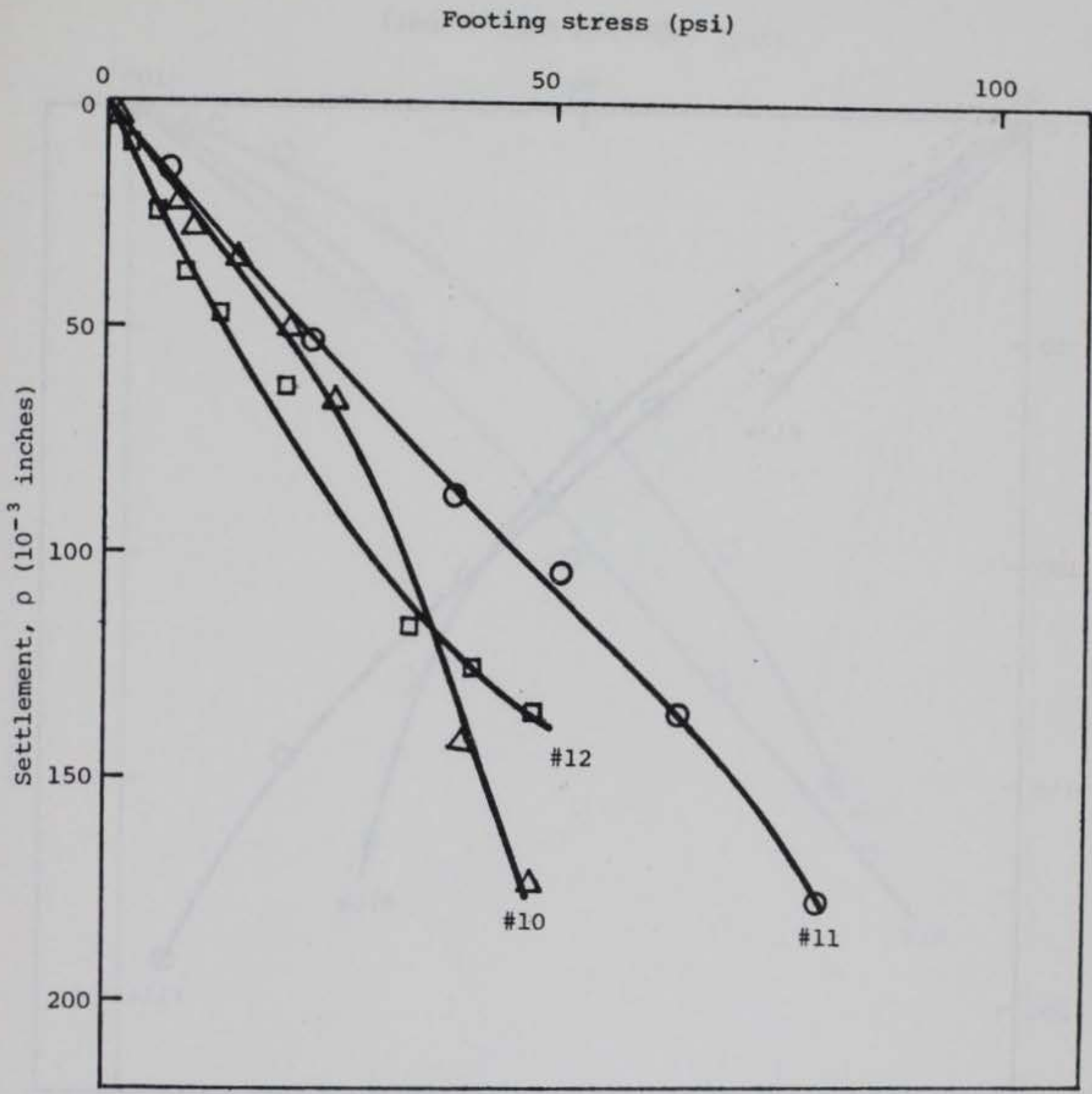
| Test No. | Radius a | a/h | $I_\rho$ | $\frac{\Delta p}{\Delta \rho}$ | E (psi) |
|---|---|---|---|---|---|
| 10 | 0.625 | 0.156 | 1.20 | 410 | 308 |
| 11 | 1.5 | 0.375 | 0.95 | 465 | 663 |
| 12 | 3 | 0.750 | 0.65 | 345 | 673 (591) |

FIG. 13   PLATE LOAD TEST RESULTS – REINFORCED SAND LAYER
          4 INCHES THICK
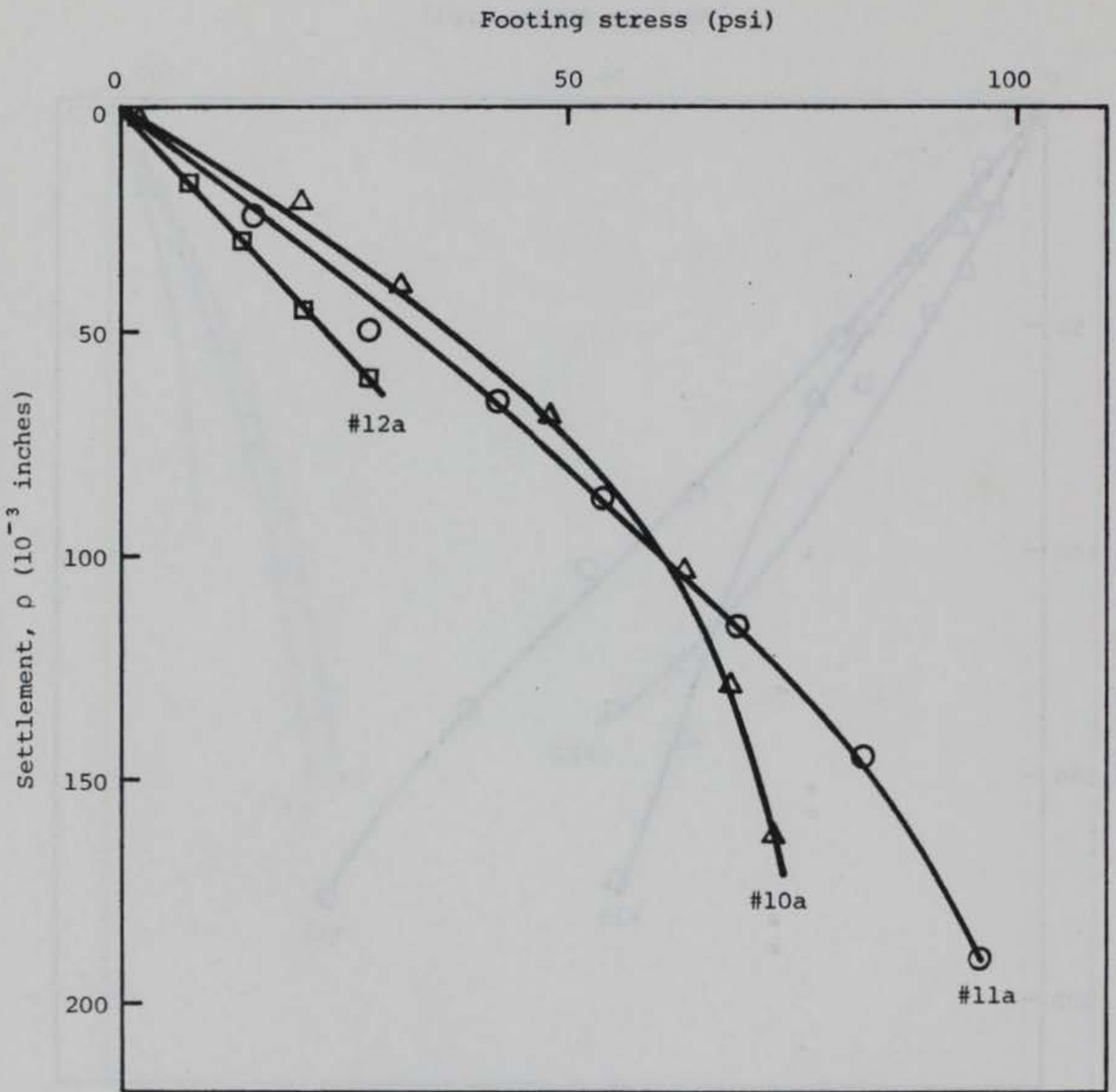
| Test No. | Radius a | a/h | $I_\rho$ | $\frac{\Delta p}{\Delta \rho}$ | E (psi) |
|---|---|---|---|---|---|
| 10a | 0.625 | 0.156 | 1.20 | 694 | 521 |
| 11a | 1.5 | 0.375 | 0.95 | 621 | 885 |
| 12a | 3 | 0.750 | 0.65 | 467 | 911 |

Footing stress (psi)
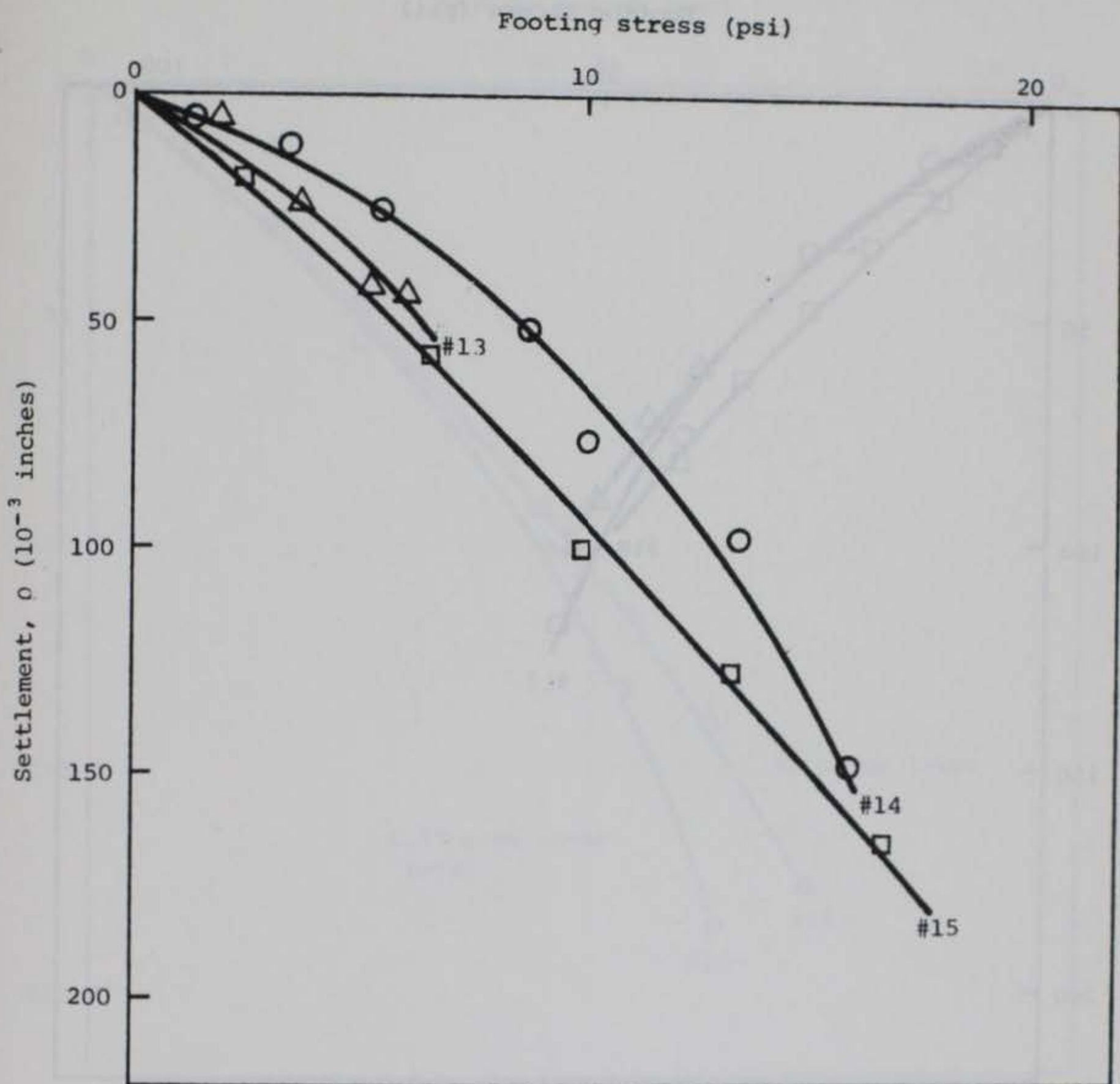
| Test No. | Radius a | a/h | $I_\rho$ | $\frac{\Delta p}{\Delta \rho}$ | E (psi) |
|---|---|---|---|---|---|
| 13 | 0.625 | 0.104 | 1.27 | 97 | 77 |
| 14 | 1.5 | 0.250 | 1.10 | 116 | 191 |
| 15 | 3 | 0.500 | 0.83 | 135 | 336 |

FIG. 14   PLATE LOAD TEST RESULTS - UNREINFORCED SAND LAYER 6 INCHES THICK

FIG. 15 PLATE LOAD TEST RESULTS - REINFORCED SAND LAYER
6 INCHES THICK
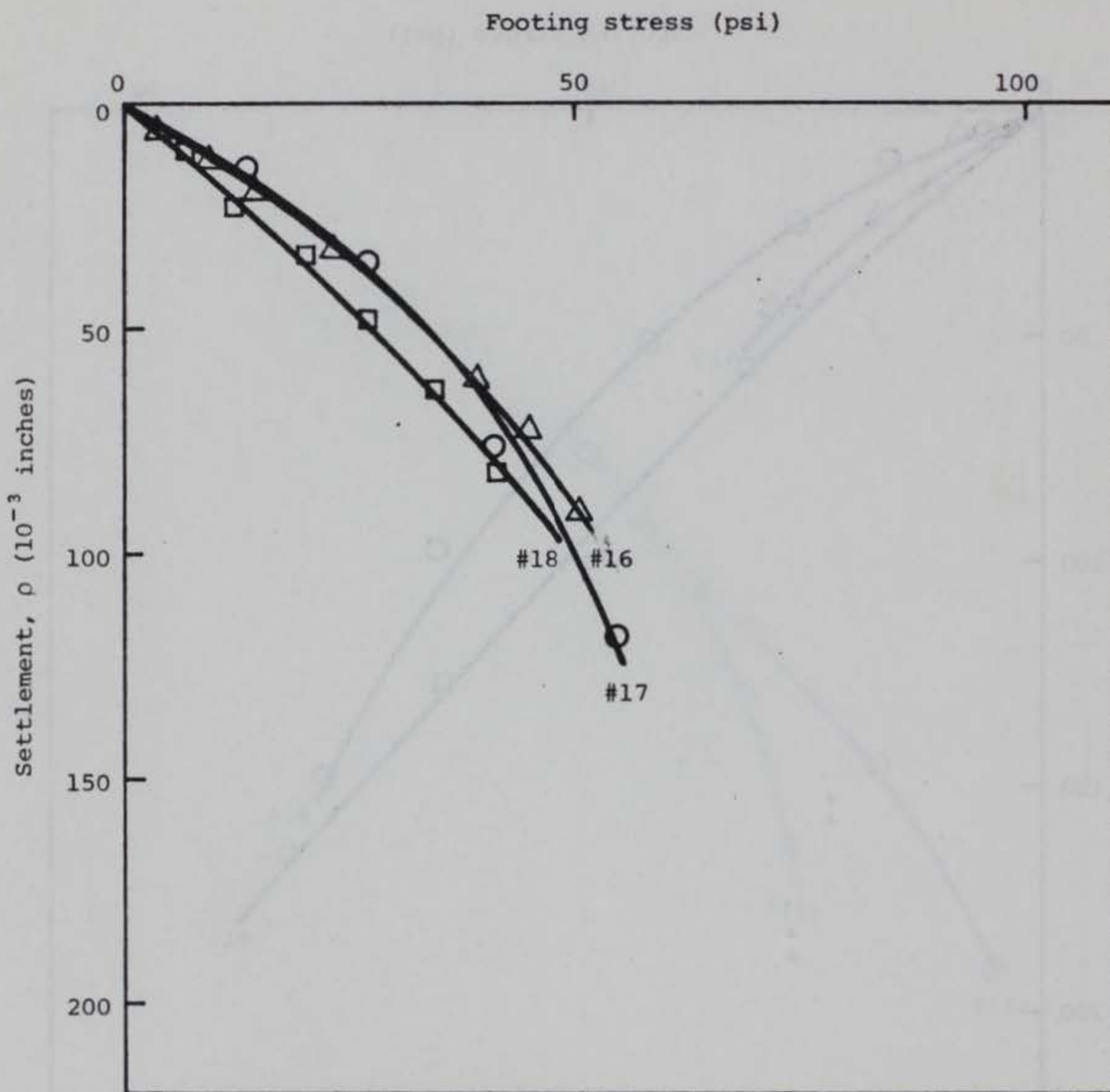
| Test No. | Radius a | a/h | $I_\rho$ | $\dfrac{\Delta p}{\Delta \rho}$ | E (psi) |
|---|---|---|---|---|---|
| 16 | 0.625 | 0.104 | 1.27 | 633 | 502 |
| 17 | 1.5 | 0.250 | 1.10 | 661 | 1090 |
| 18 | 3 | 0.500 | 0.83 | 505 | 1257 |

| Test No. | Radius a | a/h | $I_\rho$ | $\frac{\Delta p}{\Delta \rho}$ | E (psi) |
|---|---|---|---|---|---|
| 19 | 2.5 | 0.417 | 0.88 | 700 | 1540 |
| 20 | 2.5 | 0.333 | 1.02 | 600 | 1530 |
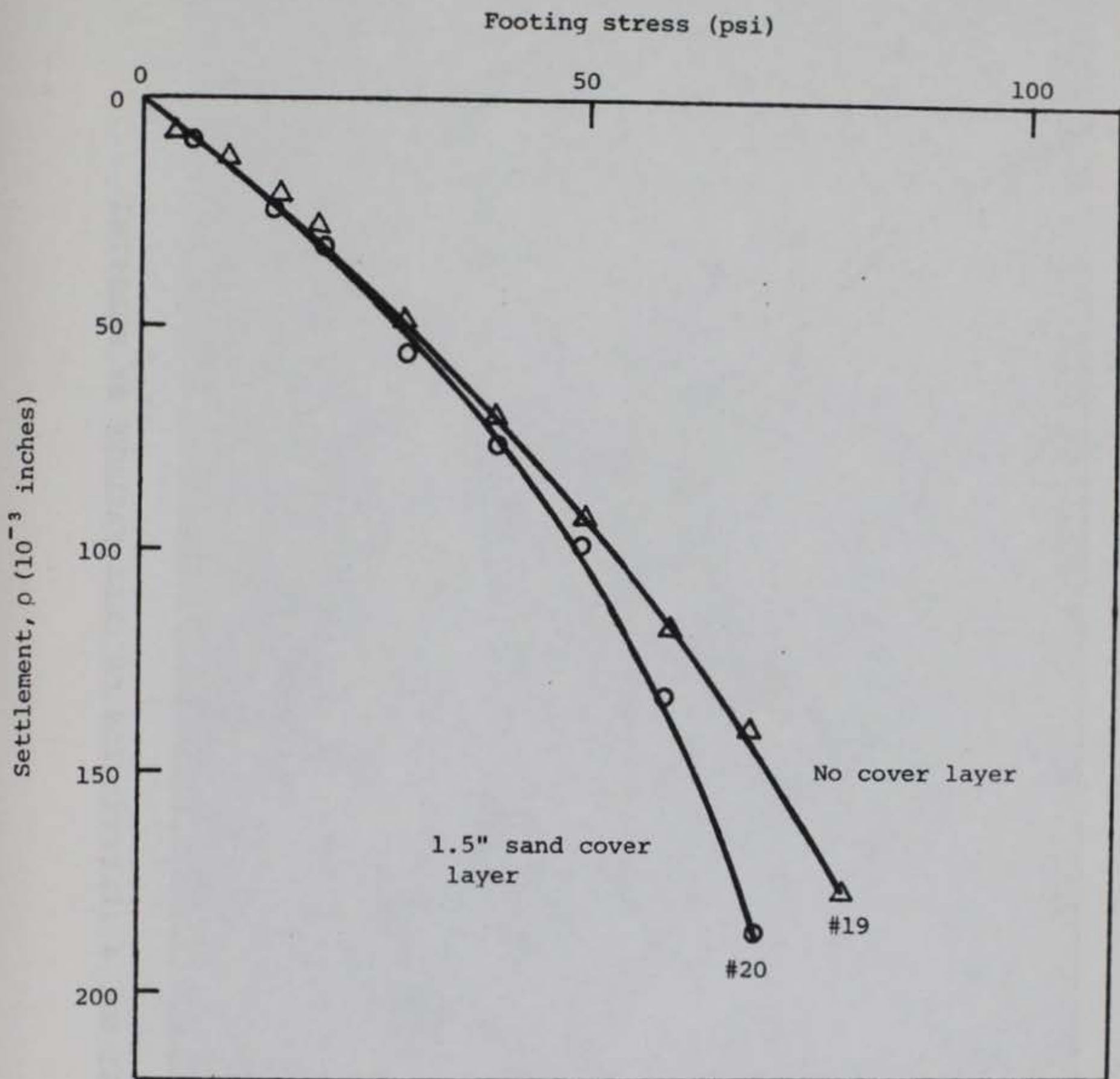
FIG. 16   PLATE LOAD TEST RESULTS – 6 INCH THICK REINFORCED SAND LAYER WITH AND WITHOUT 1.5 INCH SAND COVER LAYER
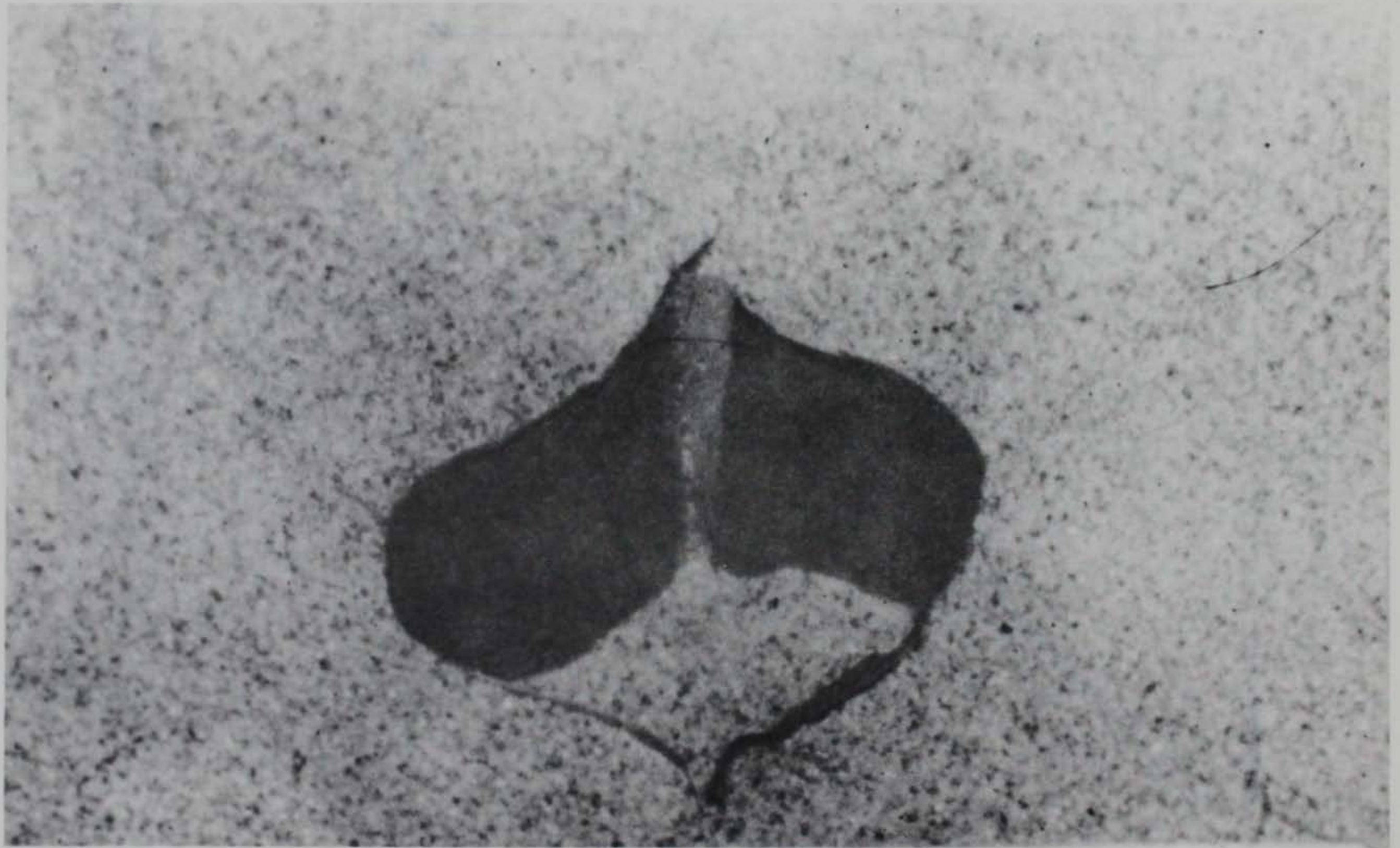
FIG. 17  TEST NO. 4 ILLUSTRATION OF CELL FAILURE BY BURSTING
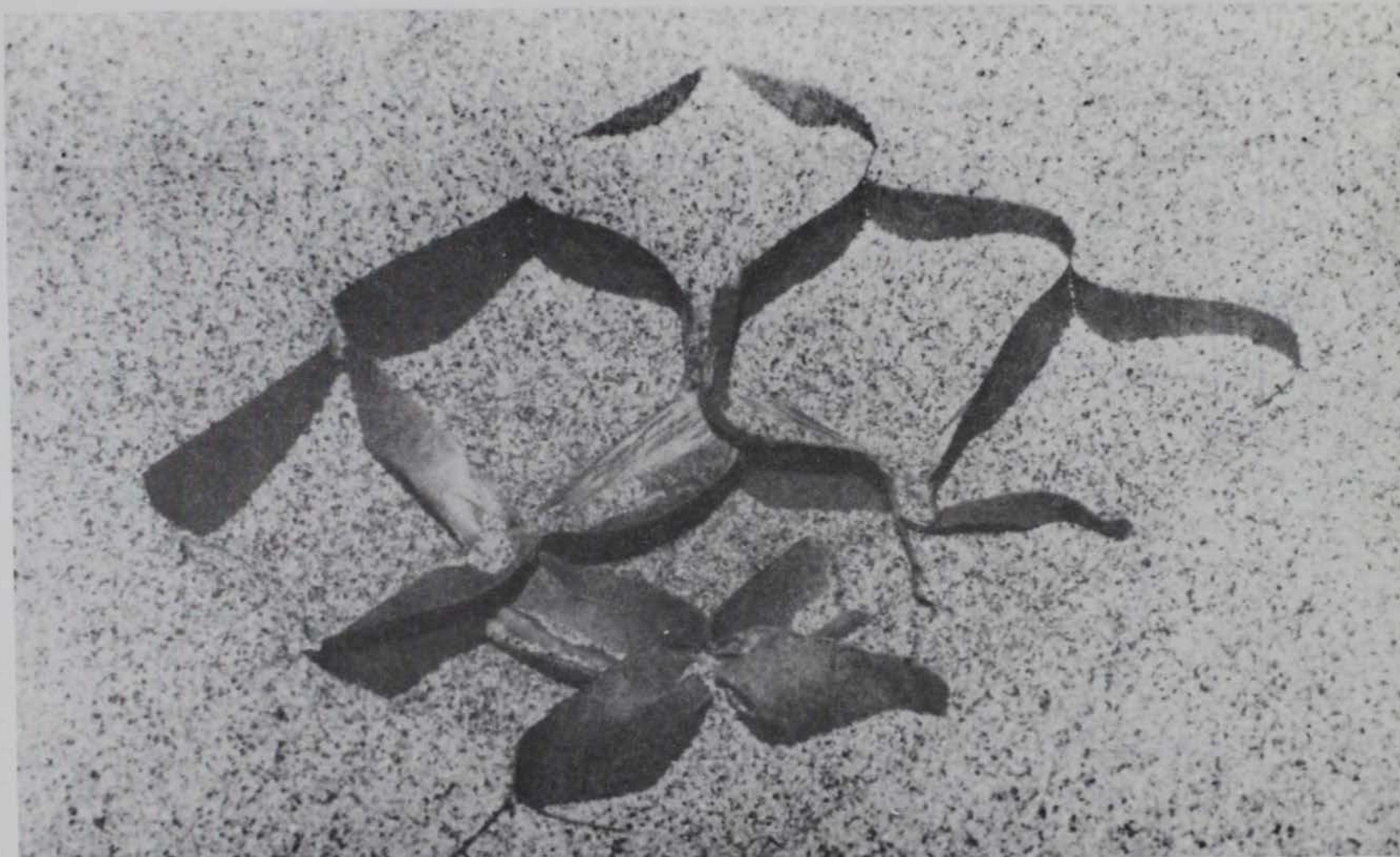
FIG. 18   TEST NO. 5 ILLUSTRATION OF CELL FAILURE BY BUCKLING
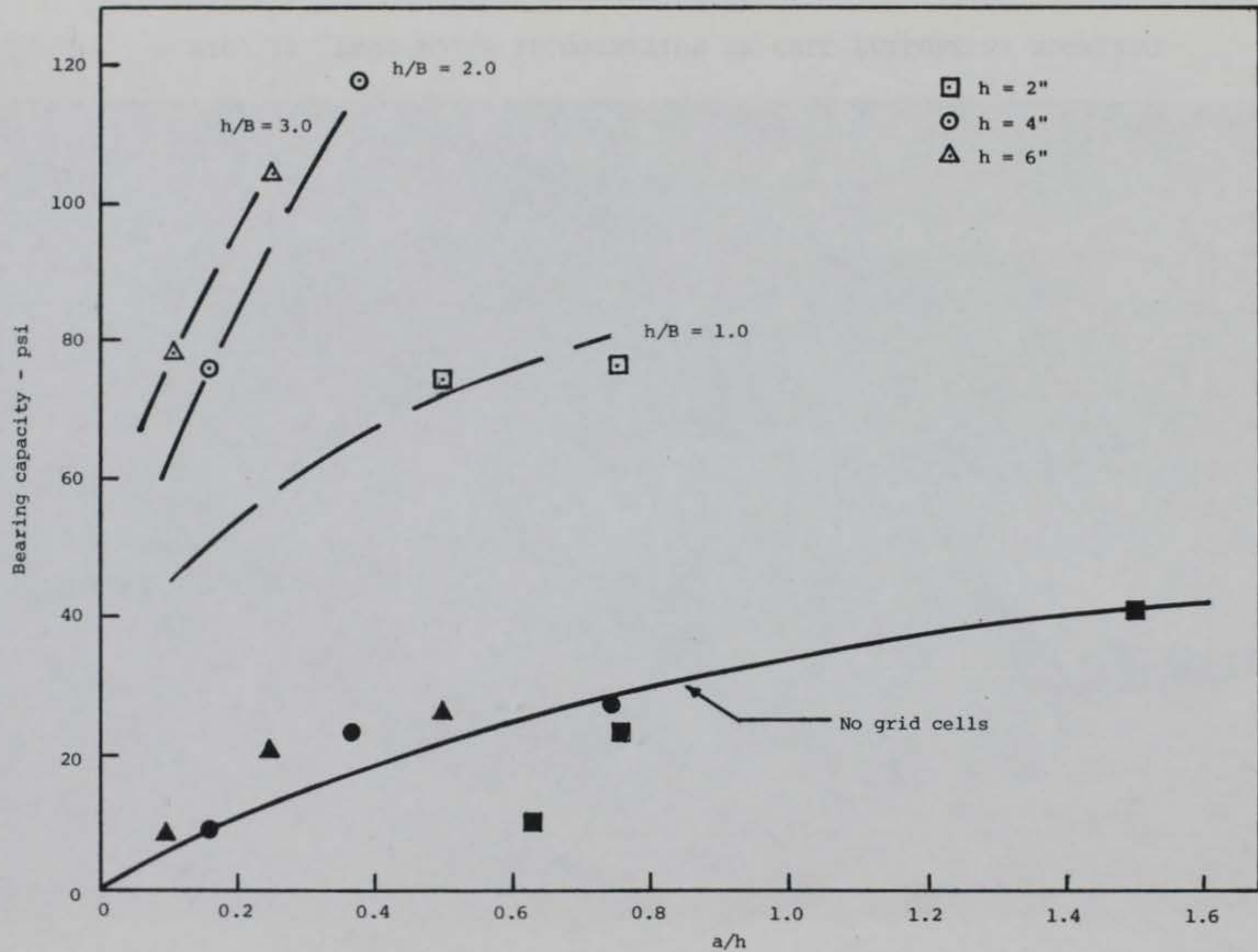
FIG. 19  BEARING CAPACITY OF UNREINFORCED AND REINFORCED SAND LAYERS OVER A RIGID BASE
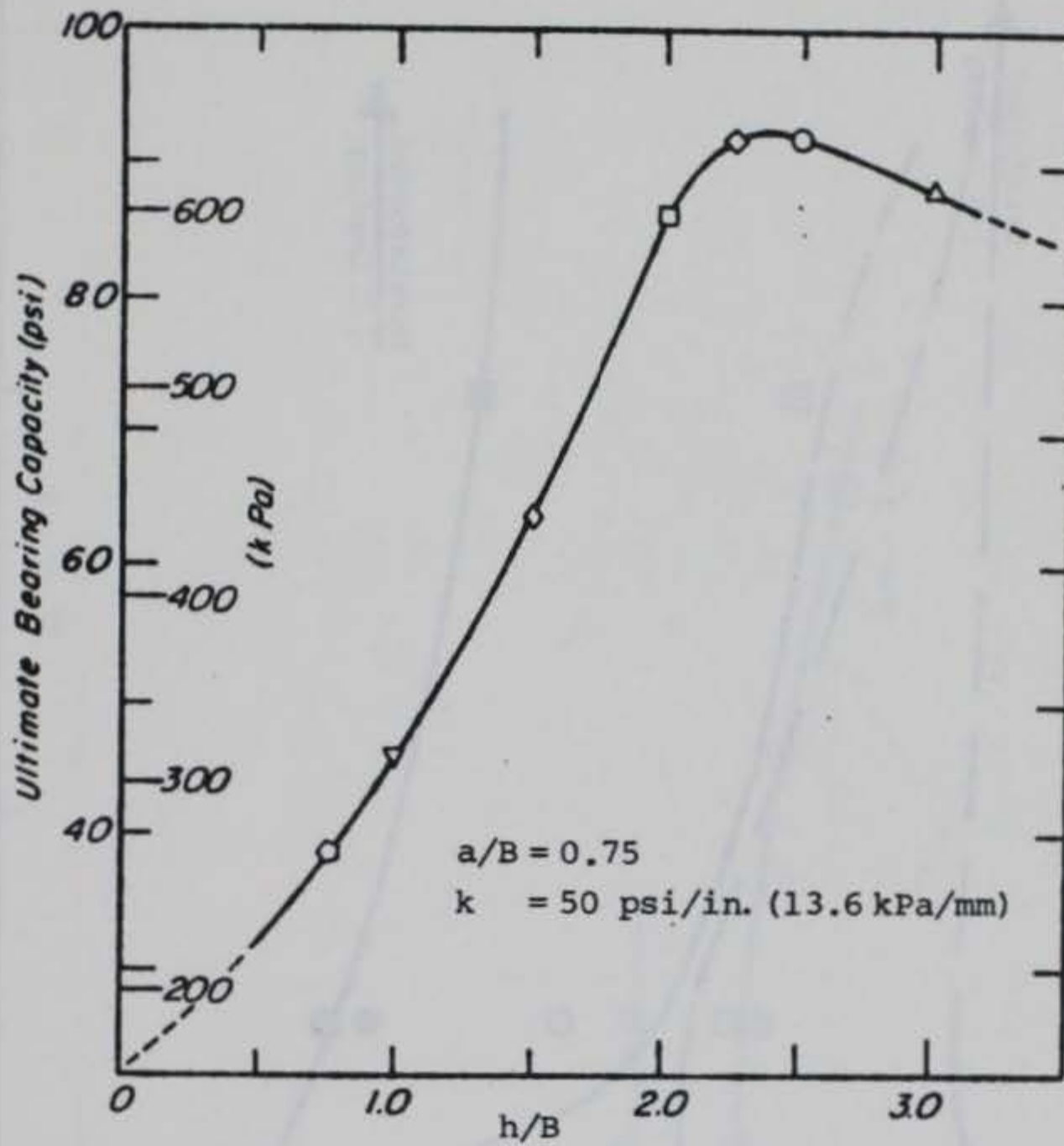
FIG. 20 EFFECT OF CELL DEPTH TO WIDTH RATIO (h/B) ON THE ULTIMATE BEARING CAPACITY OF GRID-REINFORCED SAND LAYER OVER A SOFT SUBGRADE

(Rea and Mitchell, 1978)
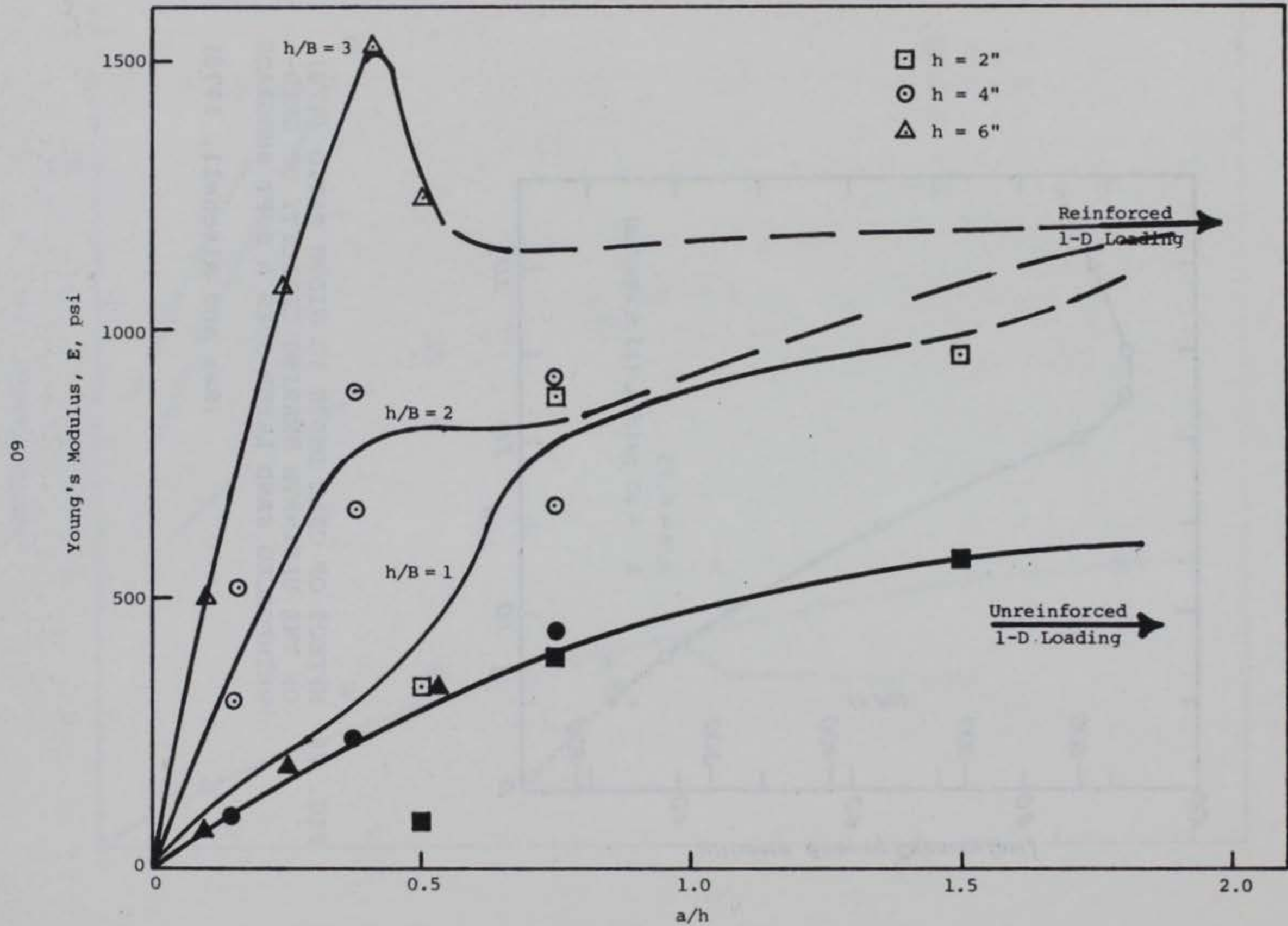
FIG. 21  VARIATION OF YOUNG'S MODULUS WITH a/h FOR UNREINFORCED AND REINFORCED SAND
LAYERS
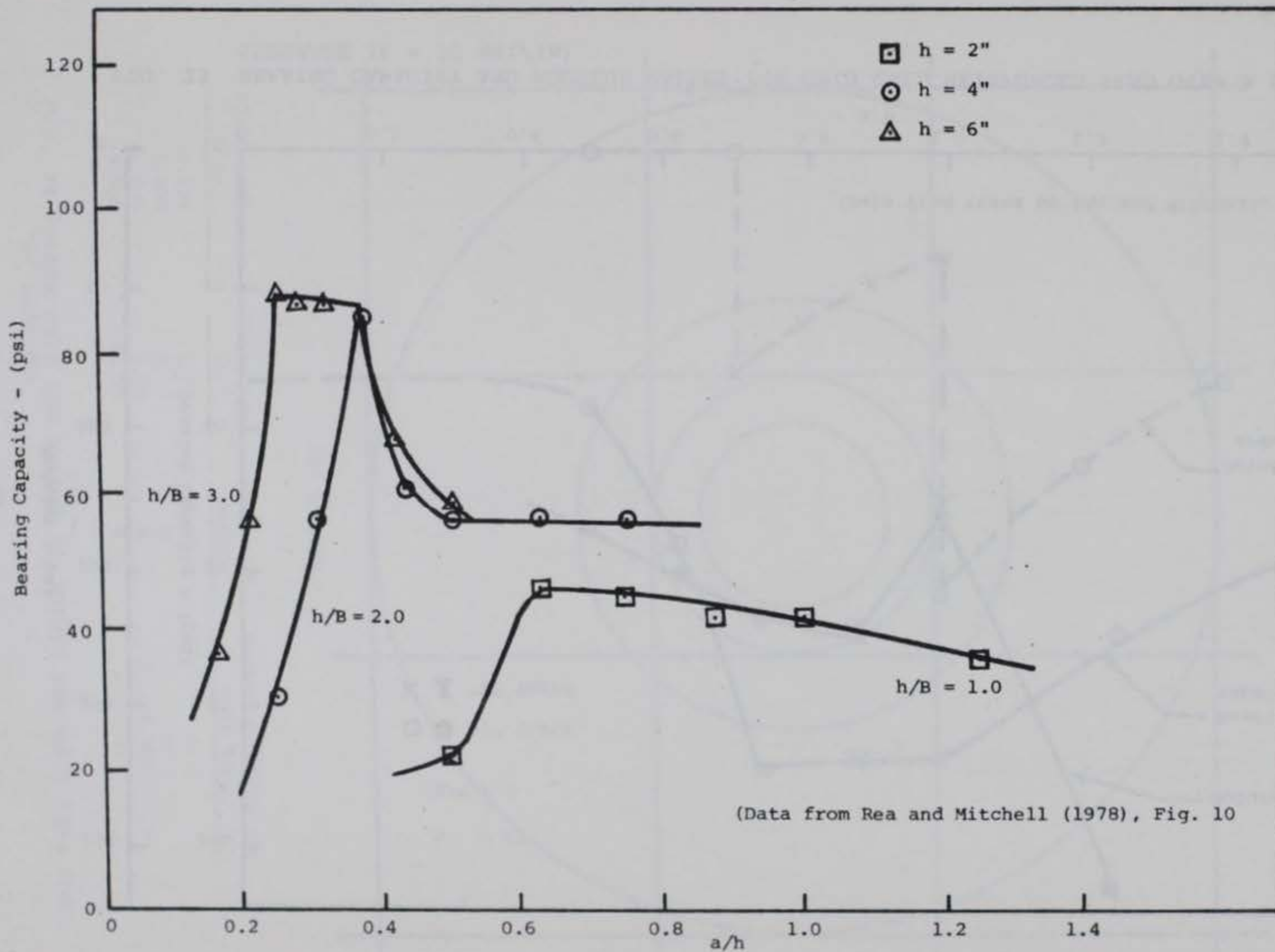
FIG. 22 BEARING CAPACITY OF GRID CELL REINFORCED SAND OVER A SOFT SUBGRADE (k = 50 psi/in)
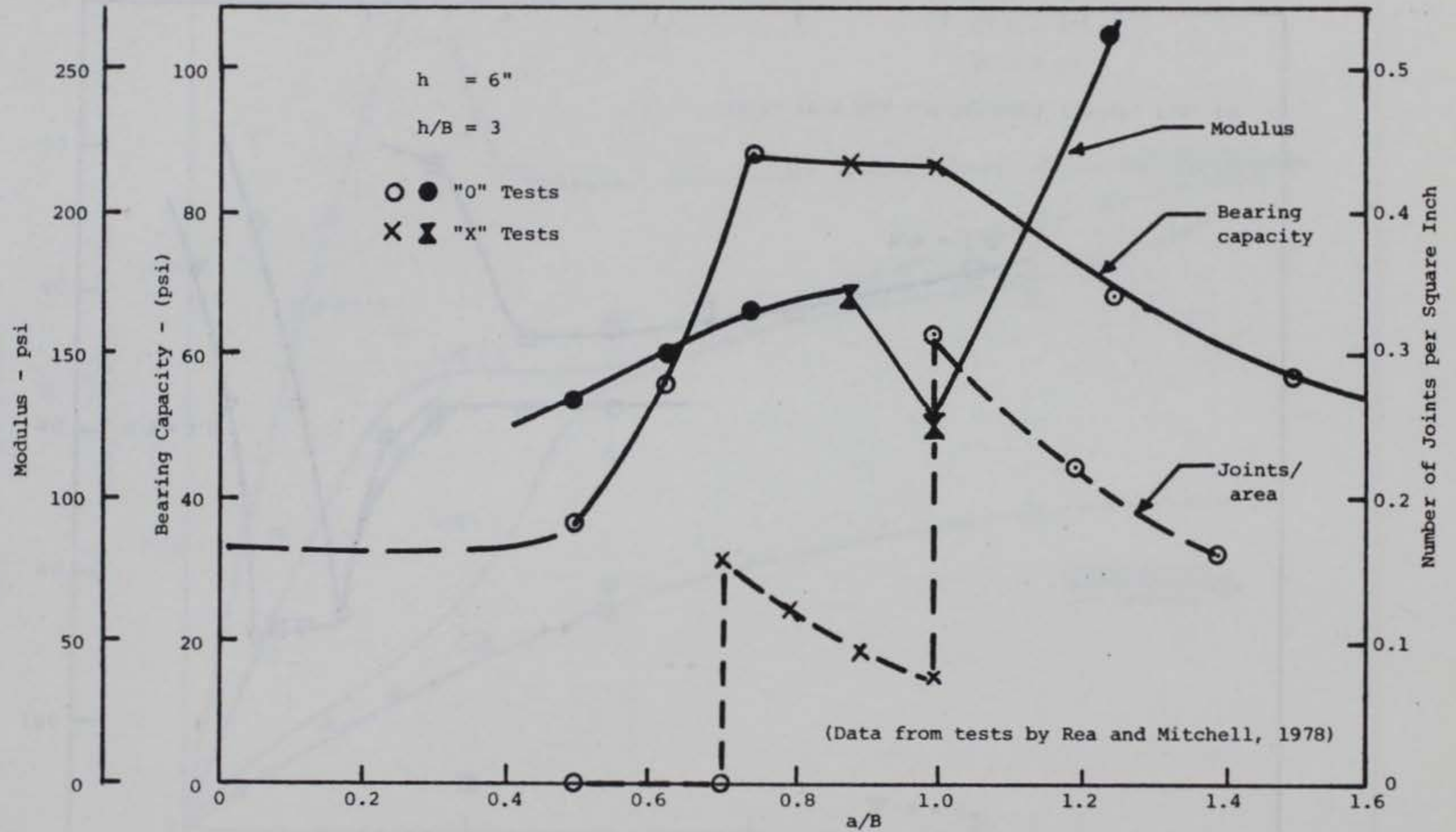
FIG. 23   BEARING CAPACITY AND MODULUS VALUES FOR GRID CELL REINFORCED SAND OVER A SOFT
SUBGRADE (k = 50 psi/in)

"0" LOADING
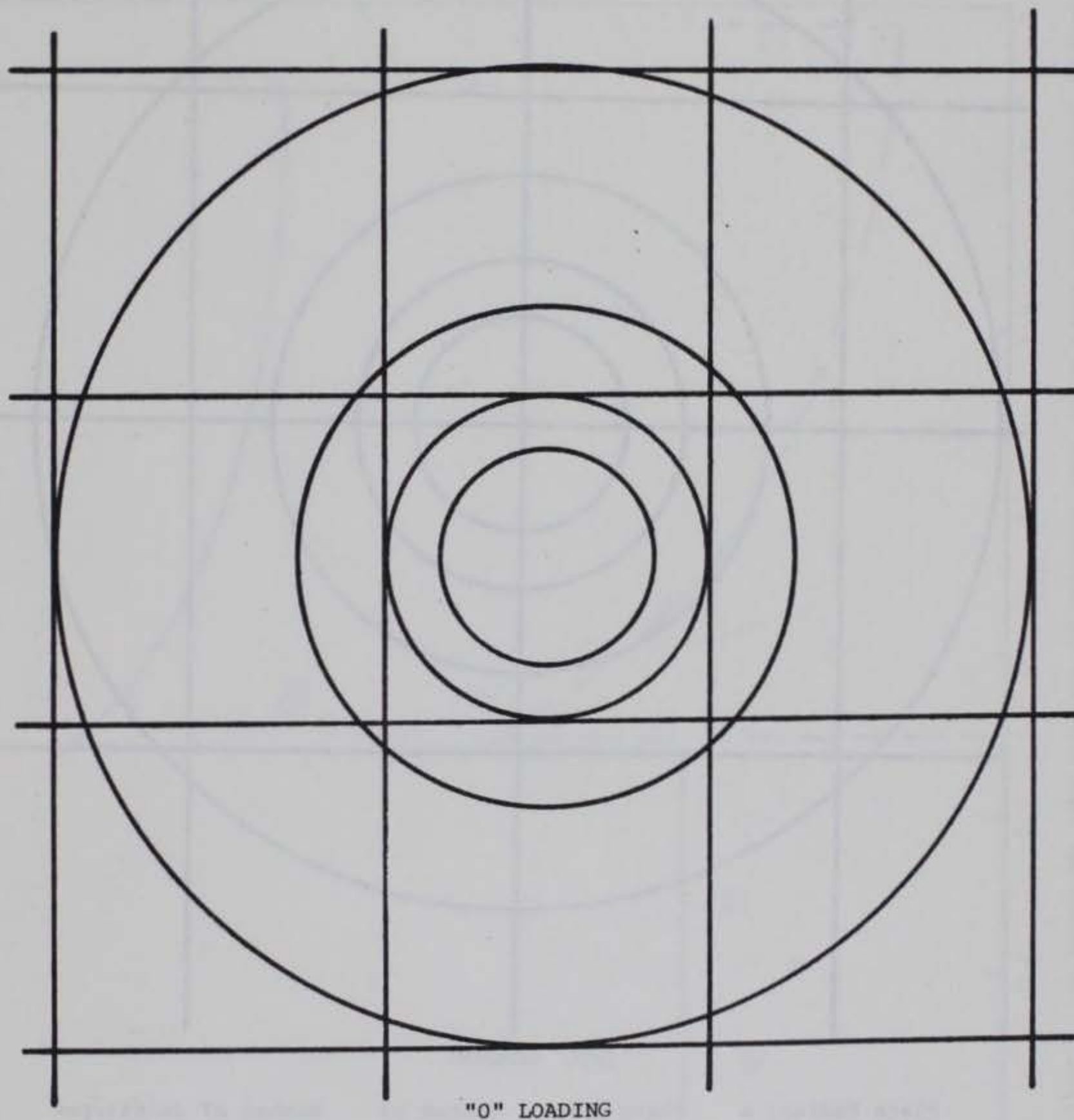
| Plate Radius, a in. | Plate Area in.$^2$ | Number of Joints | Number of Joints per Unit Area |
|---|---|---|---|
| 0.625 | 1.23 | 0 | 0 |
| 1.000 | 3.14 | 0 | 0 |
| 1.500 | 7.07 | 4 | 0.566 |
| 3.000 | 28.27 | 4 | 0.141 |

FIG. 24   PLATE SIZE AND NUMBER OF JOINTS PER UNIT AREA FOR "0" LOADING
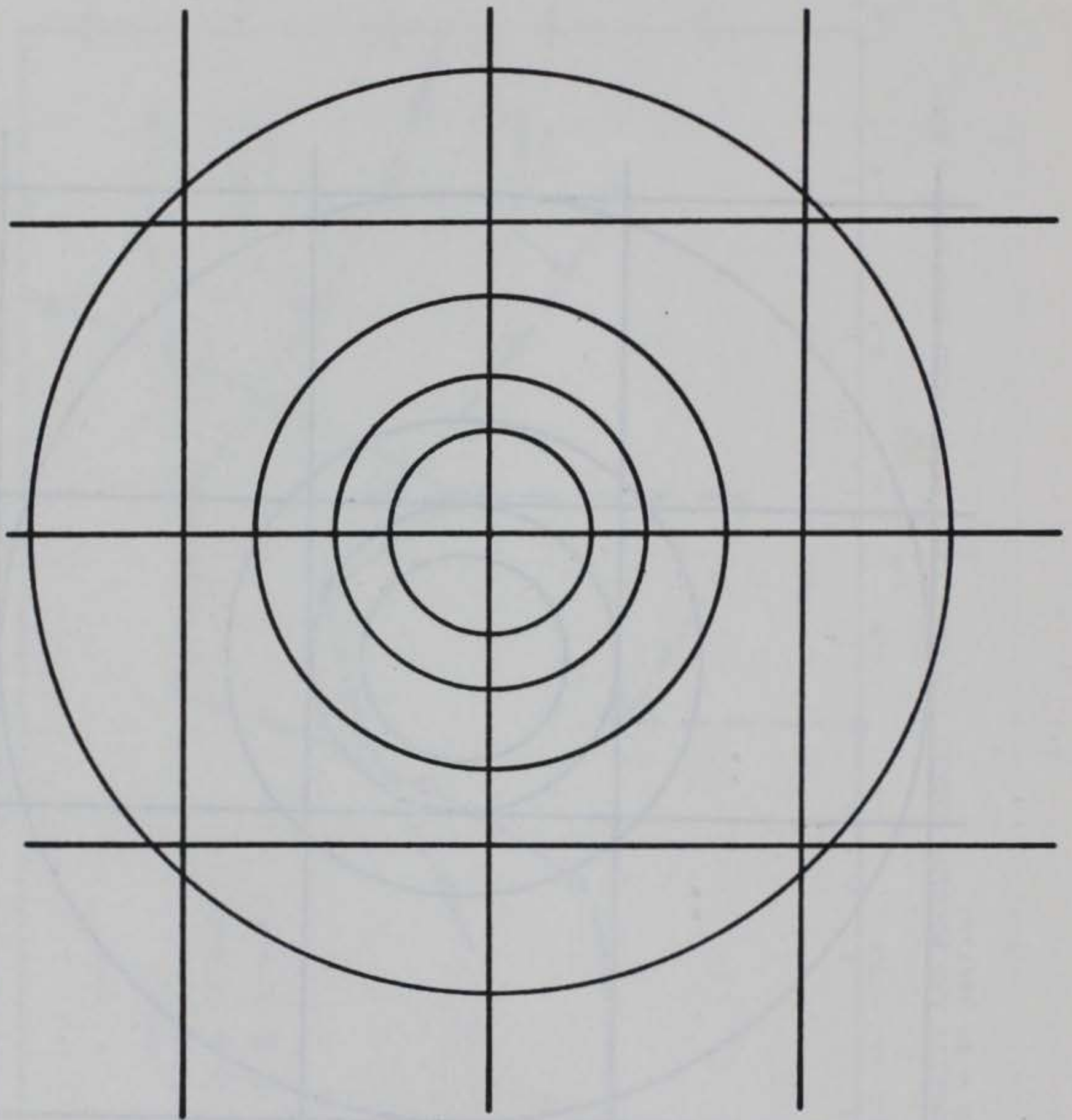
"X" LOADING

| Plate Radius, a in. | Plate Area in.$^2$ | Number of Joints | Number of Joints per Unit Area |
|---|---|---|---|
| 0.625 | 1.23 | 1 | 0.813 |
| 1.000 | 3.14 | 1 | 0.318 |
| 1.500 | 7.07 | 1 | 0.141 |
| 3.000 | 28.27 | 9 | 0.318 |

FIG. 25   PLATE SIZE AND NUMBER OF JOINTS PER UNIT AREA FOR "X" LOADING
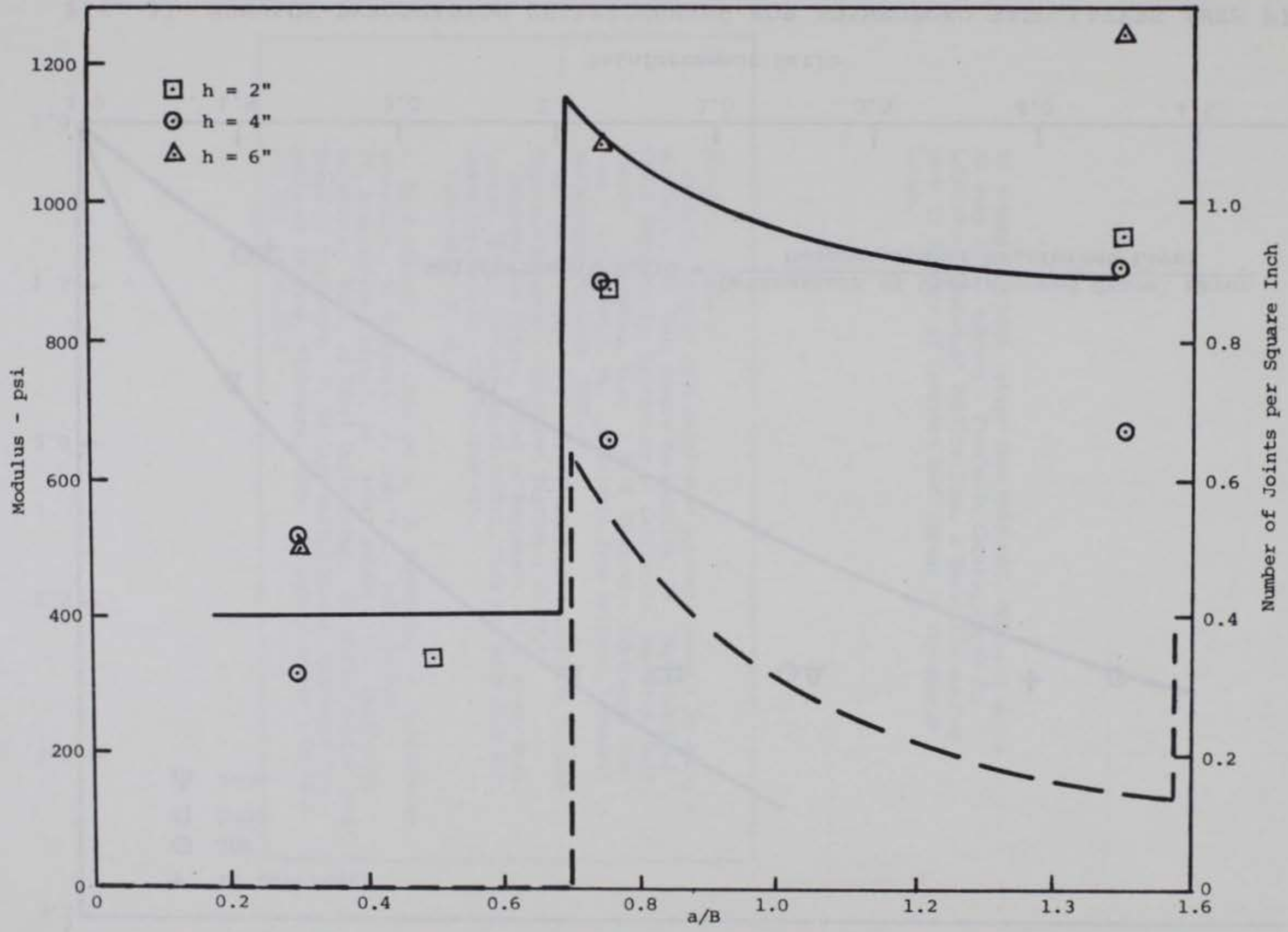
FIG. 26  VARIATION OF MODULUS AND NUMBER OF JOINTS PER UNIT AREA OF LOADING PLATE
WITH a/B
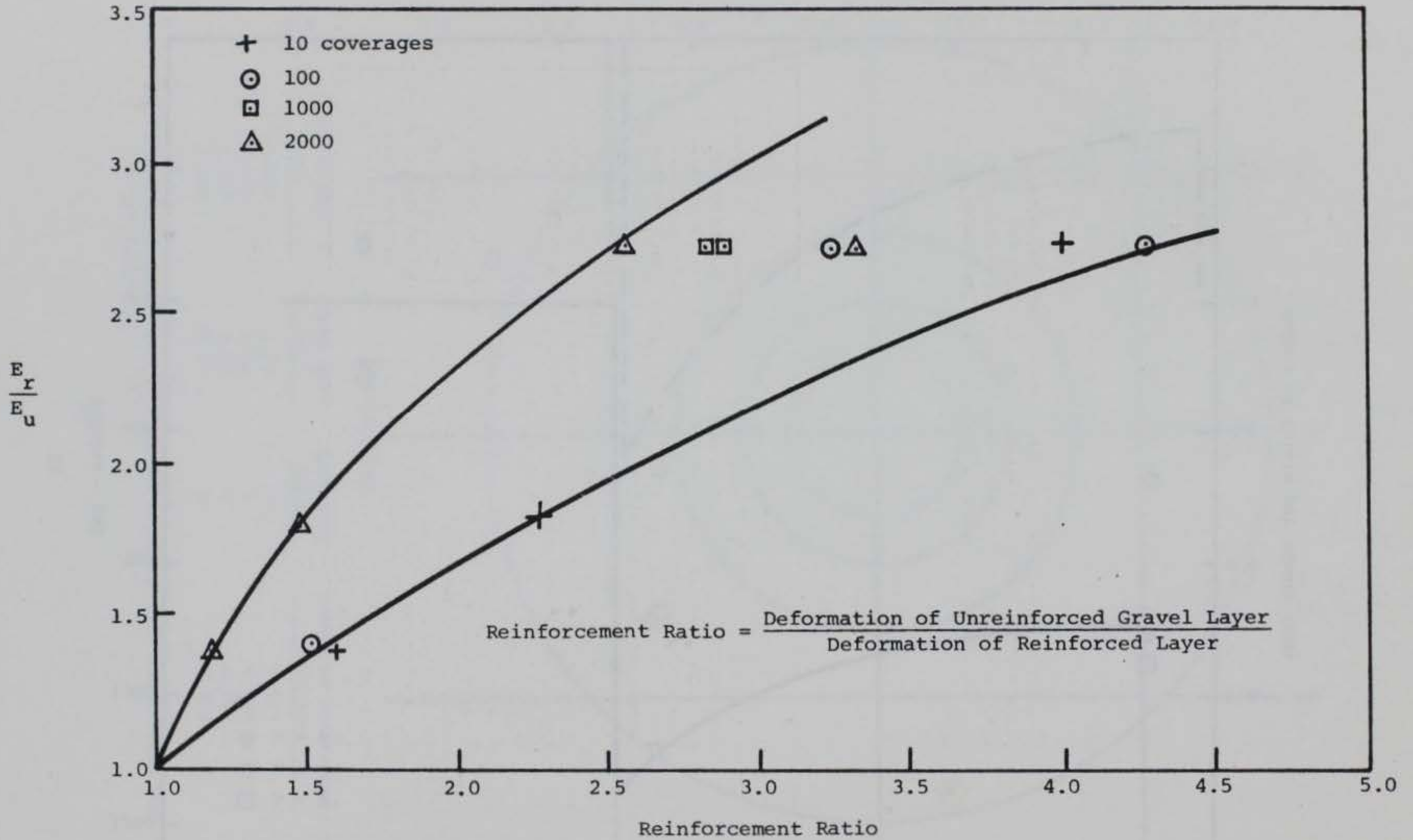
FIG. 27  MODULUS-DEFORMATION RELATIONSHIPS FOR REINFORCED SAND LAYERS (WES FIELD TESTS)

In accordance with letter from DAEN-RDC, DAEN-ASI dated
22 July 1977, Subject: Facsimile Catalog Cards for
Laboratory Technical Publications, a facsimile catalog
card in Library of Congress MARC format is reproduced
below.